

**Part A: Synthesis of gold nanoparticles using gellan gum as reducing and stabilizing agent**

**5A.1** Electrolyte conditions and pH changes has impeded the applications of AuNPs.<sup>[7]</sup> To survive *in-vitro* and *in-vivo* environment, it is necessary to have a system which is water soluble, aggregation resistant, biocompatible, does not include toxic chemicals in the synthesis protocol and also introduce functionality to the particle surface for the conjugation of biomolecules for medical applications.

The current chapter describes our initiation to synthesize and stabilize AuNPs using anionic polyelectrolyte gellan gum (GG). Until now gums such as gum Arabic<sup>[8]</sup> have been used for stabilizing colloids, but the reduction of metal to nanoparticles by the gums and their utility in drug delivery is largely a new and unexplored area. Gellan gum,<sup>[9]</sup> a high molecular weight polysaccharide gum, is produced by a pure culture fermentation of a carbohydrate by *Pseudomonas elodea*. The production organism is an aerobic, well characterized, non-pathogenic, gram-negative bacterium. Gellan gum is water soluble and is commercially available as a free flowing white powder. It is approved for food, non food, cosmetic and pharmaceutical use in the United States, Canada, Australia and many other countries in Latin America, South America, Asia and the European Union. According to the FDA, GG may be safely used as a direct food additive for human consumption as per 21 CFR 172.665 and appears as E418 in the European Community Directive. Its water solubility, thickening, gelling and stabilizing agent properties are some of the reasons for its wide application in food and pharmaceutical industry; it is currently used in bakery fillings, confections, dairy products, etc. Gellan gum is also used as an ingredient in personal and oral care applications such as hair care products, creams, sunscreens, etc. In addition to its non-toxic properties and wide acceptance within the human food chain, GG has unique structural features that attracted our attention. Its structure consists of four linked monosaccharides (i.e., simple sugars), including one molecule of rhamnose (a sugar found in various plants), one molecule of glucuronic acid (an oxidized glucose molecule) and two molecules of glucose (a component of sucrose, which is common sugar).<sup>[10,11]</sup> This part of the chapter describes the synthesis of AuNPs using GG as the reducing and stabilizing agent. The synthesized AuNPs were characterized for optical properties, morphology, zeta potential and stability under different pH and electrolytic conditions as well as long term stability.

## 5A.2 Experimental work

### 5A.2.1 Synthesis of gellan gum reduced gold nanoparticles

In a typical experiment, an aqueous solution of  $\text{AuCl}_4$  ( $10^{-4}\text{M}$ ,  $100\ \mu\text{L}$ ) was reduced to AuNPs by heating it in 0.02% w/v aqueous solution of GG (100 mL). After the addition of  $\text{AuCl}_4$ , the pH of the solution was adjusted with sodium hydroxide between the ranges 11-12 to yield ruby red AuNPs on boiling for 5 min. The AuNPs dispersion was thoroughly dialyzed (dialysis tubing 12 kDa cut off) for 24 h to remove the by products of the reaction.

### 5A.2.2 Preparation of spray dried gold nanoparticles

After preparation of gellan gum reduced gold nanoparticles (GG-AuNPs), the dispersion was dialyzed and spray dried using a laboratory scale spray dryer. During the spray drying operation, the inlet and outlet temperatures were maintained at  $100\text{--}110^\circ\text{C}$  and  $50\text{--}60^\circ\text{C}$  respectively. The atomized air pressure and aspirator was maintained at  $2\text{kg}/\text{cm}^2$  and  $-200\ \text{mm WC}$  respectively to collect the dry and free flowing product. The product was collected and stored in desiccators till further study.

### 5A.2.3 Characterization

#### 5A.2.3.A UV-Visible spectroscopy measurements

The surface plasmon resonance of gellan gum reduced AuNPs was monitored by UV/Vis/NIR spectroscopy, at a resolution of 2 nm.

#### 5A.2.3.B Transmission electron microscopy (TEM) measurement

Samples for TEM analysis were prepared by drop casting of GG-AuNPs and spray dried gellan gum reduced gold nanoparticles (SD-GG-AuNPs) on carbon coated copper grids and allowed to dry at room temperature. Measurements were taken at an accelerated voltage of 300 kV with a lattice resolution of 0.14 nm and point image resolution of 0.20 nm. The particle size analysis was carried out using Gatan software.

#### 5A.2.3.C X-ray diffraction (XRD) measurements

Samples were prepared on glass substrates by simple solvent evaporation of dispersions of GG-AuNPs for X-ray diffraction measurements operating at 40 kV and a current of 30 mA at a scan rate of  $0.38^\circ\text{min}^{-1}$ .

**5A.2.3.D Zeta potential measurements**

The surface charge of GG-AuNPs was determined by measurement of zeta potential. The average zeta potential of nanoparticles dispersion was measured as such without any dilution.

**5A.2.3.E In vitro stability studies of gold nanoparticles**

The stability of AuNPs was studied over time and under different pH and electrolytic conditions. In case of pH studies, the pH of GG-AuNPs was adjusted from pH 2-12 and incubated for 24 h at room temperature. The analysis of the characteristic absorption peak was checked for the precipitation of AuNPs. The stability of AuNPs was also tested by challenging the GG-AuNPs in the presence of electrolyte (sodium chloride) solution and incubated for 24 h before taking the absorption measurements. For long term stability study, GG-AuNPs dispersion and SD-GG- AuNPs were kept at 25<sup>o</sup>/65% RH (room temperature) and at 2-8<sup>o</sup>C (refrigerated) for a period of three months. The GG-AuNPs and SD-GG-AuNPs samples were characterized by UV/Vis spectroscopy measurements and TEM analysis.

### 5A.3 Results and discussion

We took advantage of the reducing, stabilizing and biocompatible properties of GG for the synthesis of AuNPs. The simple carbohydrates like glucose are reducing sugars that are capable of reducing gold ions ( $\text{AuCl}_4$ ) to form AuNPs.<sup>[12]</sup> It was envisaged that this strategy would render dual advantage by providing sufficient charge on the nanoparticles, which will aid in the subsequent attachment of the biomolecules for drug delivery purpose as well render optimum stability and subsequently help to improve the uptake of the nanoparticles. It is well known that AuNPs exhibit ruby red color in water and this color arises due to excitation of surface plasmon vibrations in the nanoparticles.<sup>[3]</sup> This surface plasmon resonance is due to collective oscillations of the electron at the surface of the nanoparticles (6s electrons of the conduction band for AuNPs) that is correlated with the electromagnetic field of the incoming light, i.e. the excitation of the coherent oscillation of the conduction band.<sup>[13]</sup>

For realization of GG synthesized AuNPs, GG was heated to enhance its solubility. After addition of  $\text{AuCl}_4$ , the pH was adjusted to 11 with sodium hydroxide and the solution was boiled for 5 min. The color of the solution changed from light yellow to ruby red (Figure 5A.1).

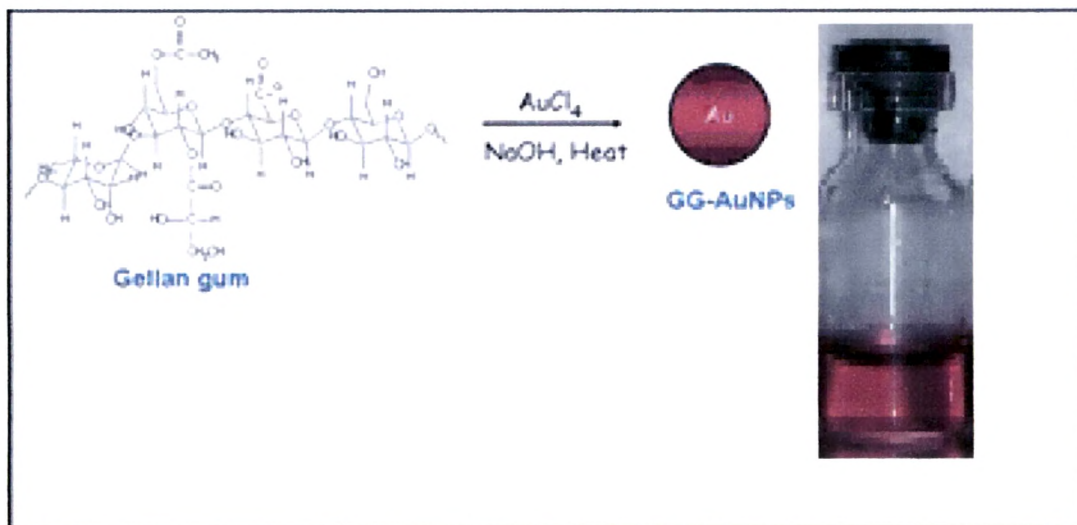


**Figure 5A.1: Synthesis of gold nanoparticles using gellan gum as reducing agent.**

Figure 5A. 2(a) shows the UVA/vis spectra recorded from the dispersion obtained by the reduction of  $\text{AuCl}_4$  using 0.02% w/v GG, the band corresponding to the surface plasmon resonance occurred at 520 nm. Surface plasmon band of AuNPs appears in the visible region and can be used to monitor shape, size and aggregation of the nanoparticles.

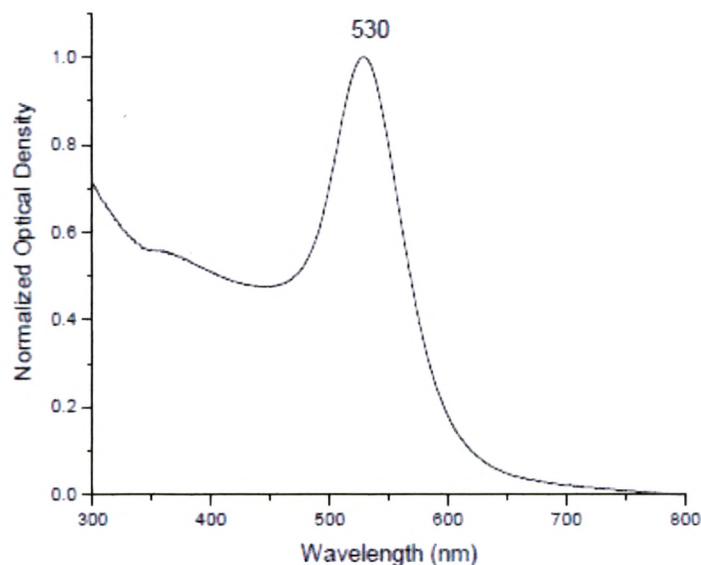
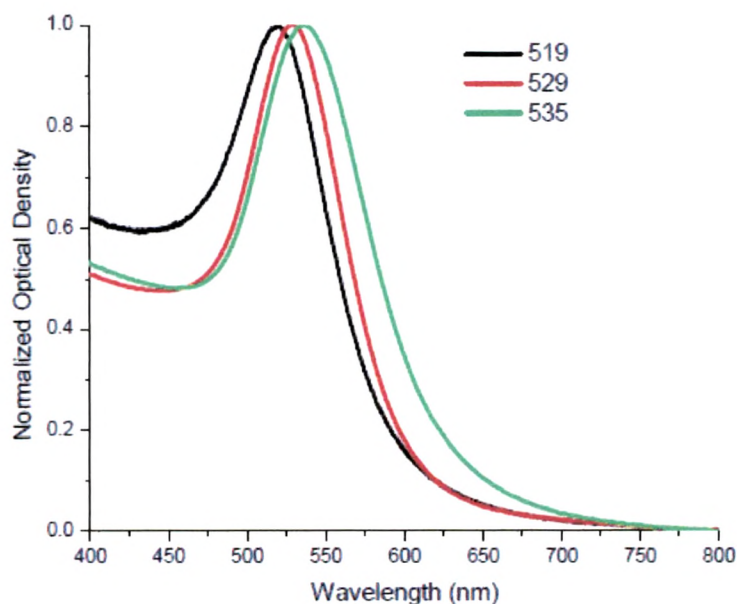


**Figure 5A.2: (a) UV/Vis absorption spectra of gellan gum (0.02% w/v) reduced gold nanoparticles.**



**(b) UV/Vis absorption spectra of gellan gum reduced gold nanoparticles measured upto 7 days.**



It was observed that  $\text{AuCl}_4$  reduction occurs rapidly and the intensity remained unchanged, without any shift in the peak wavelength even after 24 h of reduction time. There was no change in the color of AuNPs dispersion (monitored upto 7 days), indicating that reduction of gold was completed and converted to AuNPs [Figure 5A.2(b)].

To evaluate the reduction efficacy of GG, effect of various concentrations of GG and gold ions as well as the effect of pH on nanoparticles formation was studied. The information drawn from the UV/Vis spectra of nanoparticles prepared by varying the concentration of GG from 0.01% w/v to 0.1% w/v illustrated that AuNPs synthesis was possible even at very low concentration of GG. The UV/Vis spectrum is presented in figure 5A.3. Varying GG solution concentrations used for the synthesis of AuNPs demonstrated that concentration of 0.01% w/v resulted in bigger and aggregated particles. The peak position shifted to 529 nm, this is in accordance with certain reports of red shift in surface plasmon resonance maxima in larger particles.<sup>[14]</sup> The surface plasmon resonance for 40 nm gold nanosphere comes at around 530 nm.<sup>[14]</sup> However at concentrations of 0.02% w/v and above, no shift in peak resonance was seen indicating the formation of AuNPs. In all the spectra, no other peaks were observed which confirms the complete formation of AuNPs and the formed nanoparticles were free of aggregation.

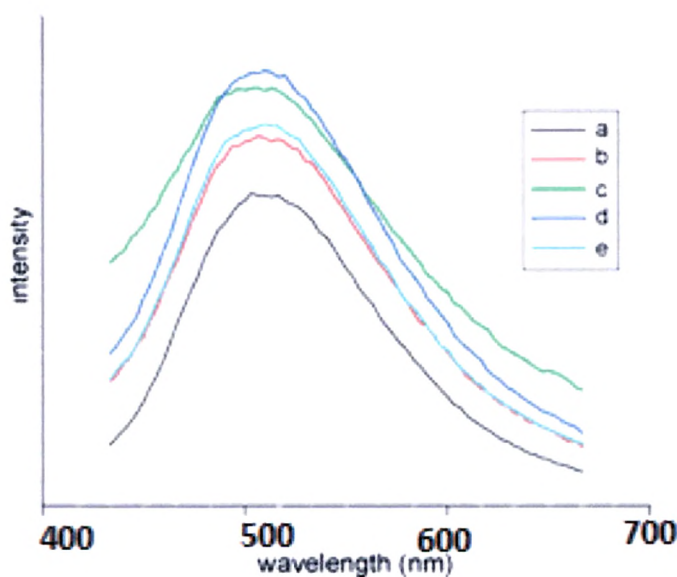


**Figure 5A.3: UV/Vis absorption spectra of gold nanoparticles synthesized using different concentrations of gellan gum.**

The concentration of gold ions also plays an important role in the synthesis of AuNPs. Influence of different concentrations of gold ions was evaluated to see the effect on the formation of AuNPs [Figure 5A. 4(a)],

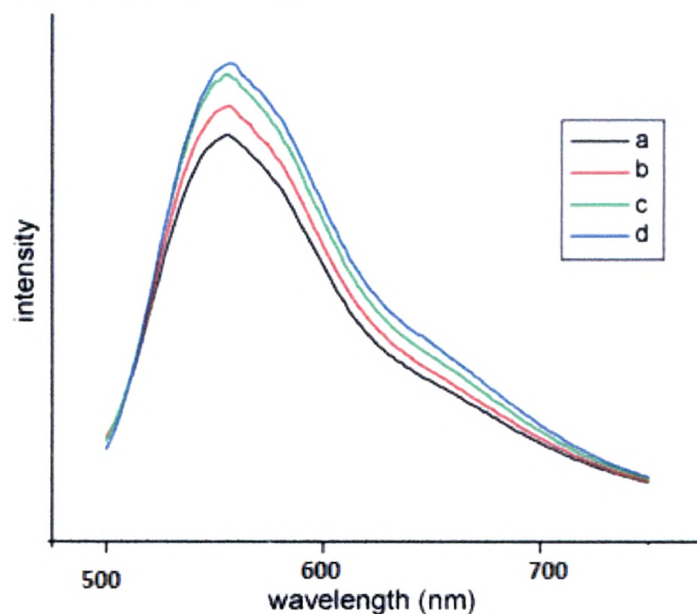
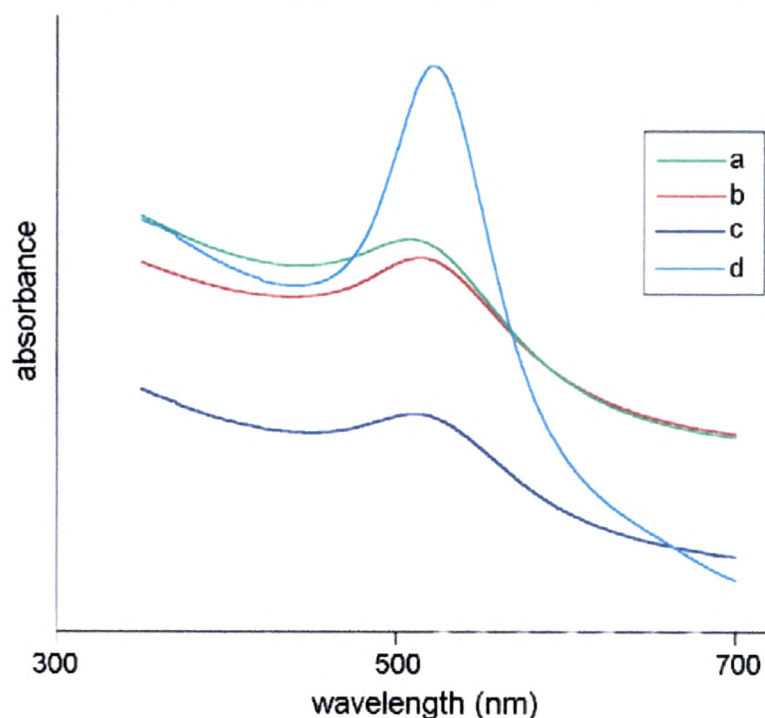


**Figure 5A.4: (a) UV-Vis absorption spectra of gellan gum (0.02% w/v) reduced gold nanoparticles using gold ion concentration of  $10^{-3}$  M.**



**(b) UV-Vis absorption spectra of gellan gum reduced gold nanoparticles synthesized at various pH (data shown after 24 h of synthesis).**

It was observed that gold ion concentrations of  $10^{-4}$  M were able to form stable, non-aggregated nanoparticles [Figure 5A. 2(a)], at gold concentration of  $10^{-3}$  M, there was no immediate formation of nanoparticles. The color of the dispersion gradually changed from light yellow to light ruby red indicating slow reduction of AuNPs [Figure 5A. 4(a)]. The surface plasmon resonance peak of AuNPs was at 537 nm (0 h), which may be due to formation of large and aggregated nanoparticles. The change in the UV/Vis spectra and color was observed upto seven days of synthesis. After seventh day, the surface plasmon peak shifted to 550 nm and the color changed from ruby red to dark purple. It was observed that at higher concentrations of gold ions, AuNPs dispersion turns purple colored with extended plasmon band, which is due to the strong interparticle interaction among aggregates.<sup>1151</sup> The UV/Vis absorption correlated well with the color change of the AuNPs. To study the effect of pH on the synthesis of AuNPs, the pH of the solutions containing GG and AuCl<sub>4</sub> were adjusted from 5 to 11 [Figure 5A. 4(b)]. The initial observation was that the simple addition of gold ions to GG solution did not result in formation of any nanoparticles. No synthesis of AuNPs occurred at pH 5 as observed by UV/Vis spectra. The spectral position of AuNPs increased slightly with increase of solution pH from 6.0 to pH 9.0. However, gold colloids of pH 6.0 to pH 9.0 exhibited a red-shift (575 nm) with a significant reduction of peak intensity, which might be due to heavy agglomeration of nanoparticles. Adjusting the pH of the solution towards basic resulted in the formation of AuNPs. As shown in [Figure 5A. 4(b)], the spectral position of AuNPs at pH 10 was 530 nm compared to 520 nm at pH 11. There was change in peak position with increase in solution pH from 10.0 to 11.0. It was clear that alkaline medium was necessary for the reduction of AuCl<sub>4</sub> by GG. Thus the pH 11 was considered as optimum for the synthesis of AuNPs.



TEM observations were employed to clarify the morphology and structure of formed AuNPs. TEM images and respective particle size distribution of AuNPs reduced by different concentration of GG are illustrated in figure 5A. 5.

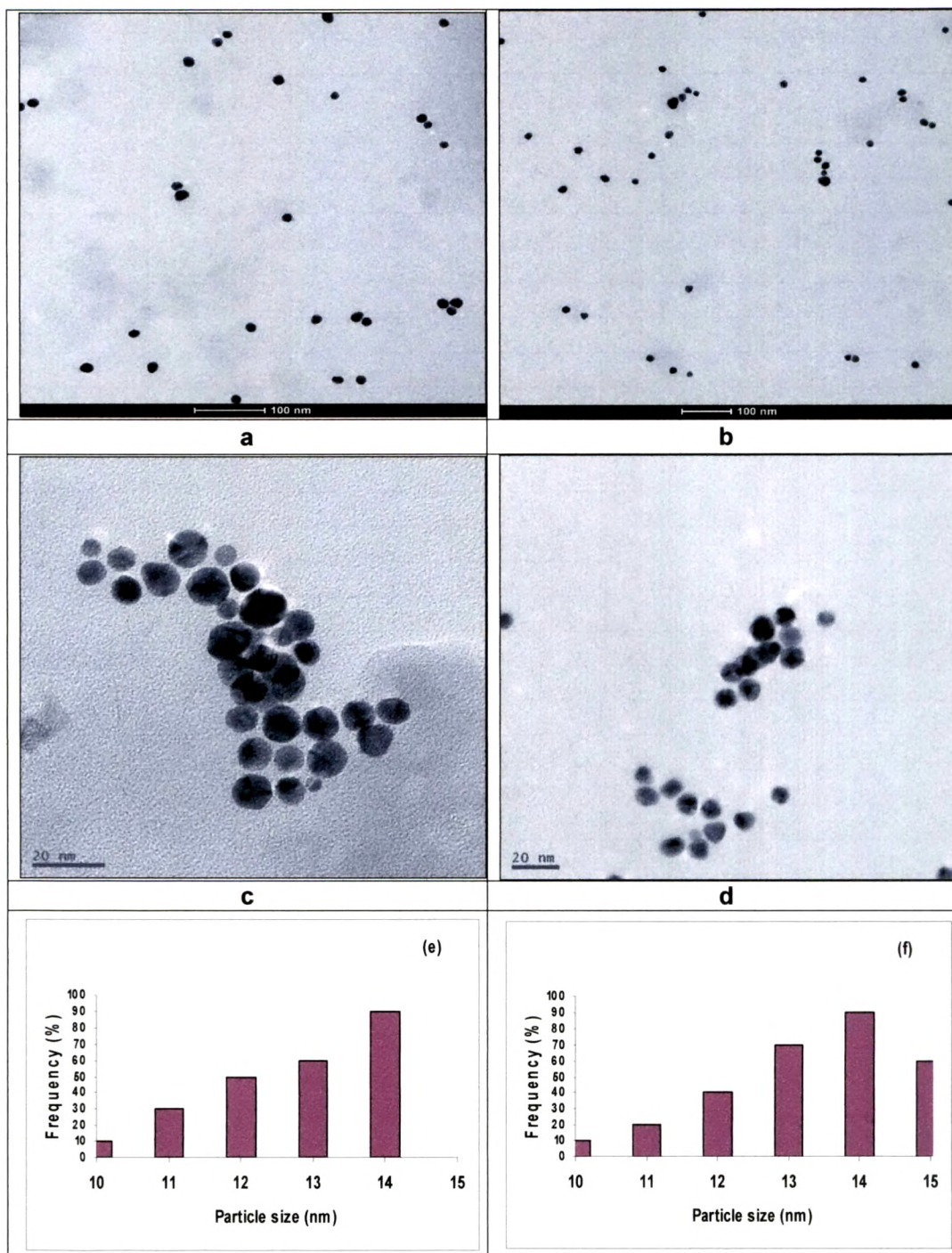


**Figure 5A.5: TEM images of (a) 0.01% w/v, (b) 0.02% w/v, (c) 0.06% w/v and (d) 0.1% w/v and particle size distribution (e) 0.02% w/v, (f) 0.1% w/v of gold nanoparticles reduced using different concentrations of gellan gum.**

As seen from the TEM image of AuNPs, almost all of the AuNPs were spherical in shape and well dispersed. However when lower concentration of CG was used as reducing agent (0.01%), it resulted in aggregated nanoparticles [Figure 5A. 5(a)]. Changes in particle size and size distribution of AuNPs with the concentration of GG may be decided by the role GG plays, the controller of nucleation or the stabilizer. When the concentration of GG was low (0.01% w/v), only few GG molecules worked as stabilizer by adsorbing on the surface of AuNPs, which resulted in the formation of large aggregated AuNPs. Gold nanoparticles prepared with relatively high concentration of GG have higher stability. Upon further increase in the concentration of GG (0.02% w/v to 0.1% w/v), no obvious changes in particle size were observed. These results illustrated the formation of monodispersed and spherical AuNPs. The electrostatic attractive forces between GG and  $\text{AuCl}_4$  in solution provide an effective driving force in formation and stabilization of nanoparticles. The size distribution of AuNPs synthesized from different concentrations of GG illustrated that at 0.01% w/v GG reduced AuNPs resulted in aggregated nanoparticles, but with increase in the concentration of GG (0.02% w/v to 0.1% w/v), the size distribution revealed that the AuNPs had a significantly narrow size distribution with an average size of 14 nm [Figure 5A. 5(e)]. It is reported that Au nanosphere having absorption maxima at 520 nm in water have an average particle size of 10 nm.<sup>[16]</sup>

To elucidate the cause of aggregation at lower GG concentrations, zeta potential measurements were carried out. The measurement of zeta potential allows predictions about stability of colloidal aqueous dispersions. Usually, particle aggregation is less likely to occur for charged particles with optimum zeta potential ( $\zeta > 30$  mV) due to electrostatic repulsion.<sup>[17]</sup> The zeta potential values of AuNPs synthesized using different concentrations of GG are given in table 5A. 1. The zeta potential measurement revealed that at lower concentrations (0.01% w/v) of GG, the values were below - 30 mV. This indicated that the coating/wrapping of the AuNPs with the anionic GG resulted in the negatively charged surface. At lower concentration the charge rendered was insufficient and leads to sensitization of the particles causing aggregation, also evidenced in TEM images [Figure 5A. 5(a)]. However, at higher concentration (0.02% w/v), sufficient charge (- 38.25 mv) was rendered making them electrostatically stable.<sup>[18]</sup> These results were in agreement with the results obtained from UV/Vis and TEM analysis.

**Table 5A.1:** Zeta potential of gold nanoparticles synthesized using different concentrations of gellan gum.

S. No.	Gellan gum concentration (% w/v)	Zeta potential (mV) of gellan gum reduced gold nanoparticles
1.	0.01	- 25.20
2.	0.02	- 38.25
3.	0.04	- 39.76
4.	0.06	- 46.88
5.	0.1	- 49.28

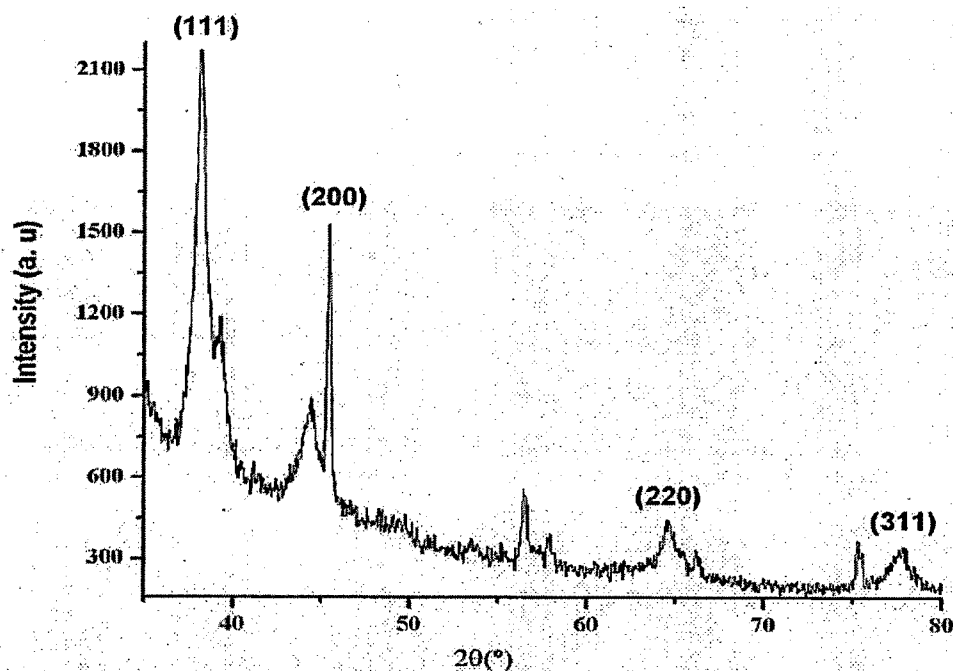
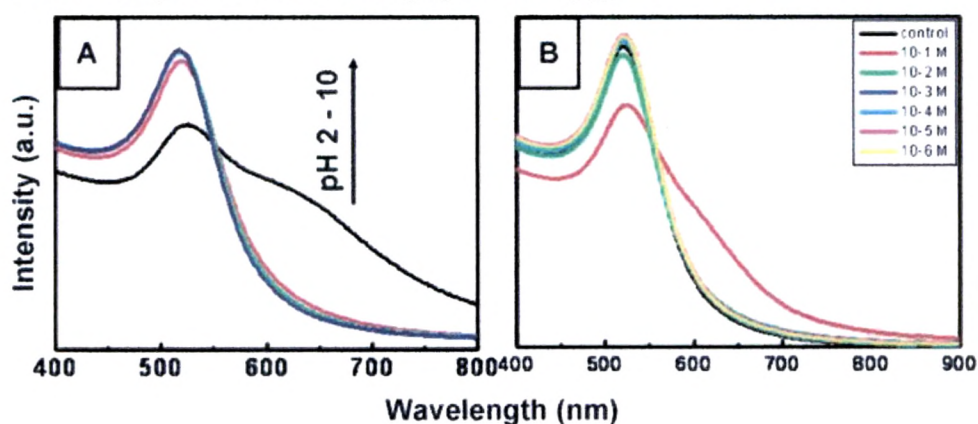


Figure 5A.6 shows the XRD patterns obtained for AuNPs synthesized using 0.02% w/v gellan gum.



A number of Bragg reflections corresponding to the (111), (200), (220) and (311) sets of lattice planes were observed which may be indexed based on the face- centered-cubic (fcc) structures of gold. The XRD pattern thus clearly showed that the AuNPs reduced by GG were crystalline in nature.<sup>[19]</sup>

A very important stipulation for the biomedical applications of nanoparticles is their stability over time and under different pH and electrolytic conditions.<sup>[7]</sup> We studied the stability of AuNPs by monitoring the surface plasmon resonance over reasonable period of time and under different pH and electrolytic conditions. It should be noted that a red shift in UV/Vis spectra is associated with either an increase in the mean size of the particles or aggregation of nanoparticles or a combination of both.<sup>[20]</sup> In case of pH study, the pH of AuNPs dispersion was adjusted from pH 2-12 using hydrochloric acid and sodium hydroxide. The sample was incubated over night and analyzed for any change in the surface plasmon resonance [Figure 5A. 7(a)],



A) pH studies B) Salt studies of Gold Nanoparticles



**Figure 5A.7:** UVVis absorption spectra of gellan gum (0.02% w/v) reduced gold nanoparticles (a, c) pH study and (b) electrolyte study.

After adjusting the pH of the AuNPs dispersion to 2, the AuNPs immediately precipitated out, this was clearly evident by the change in the intensity and position in the UVA/vis spectra. There was an additional peak around 650 nm. The color of the dispersion also changed from ruby red to purple [Figure 5A. 7(c)], Gold nanoparticles dispersion did not show any discernible change in the intensity or position at  $\sim 520$  nm in the pH window of 4-12. Even the addition of sodium chloride upto  $10^{-1}$  M caused no major aggregation in the AuNPs [Figure 5A. 7(b)]. As the surface plasmon resonance position is very sensitive to aggregation, the minimal change in its position under the above experimental conditions indicates the extra stability of GG stabilized AuNPs. Other AuNPs systems obtained by borohydride or citrate reduction routes aggregate at the slightest change in their pH and electrolyte environments.<sup>[7]</sup>

The long term stability of nanoparticles was also monitored by keeping nanoparticles dispersions under stabilized conditions of 25°C/65% RH (room temperature) and 2-8°C (refrigerated) for three months (Figure 5A. 8).

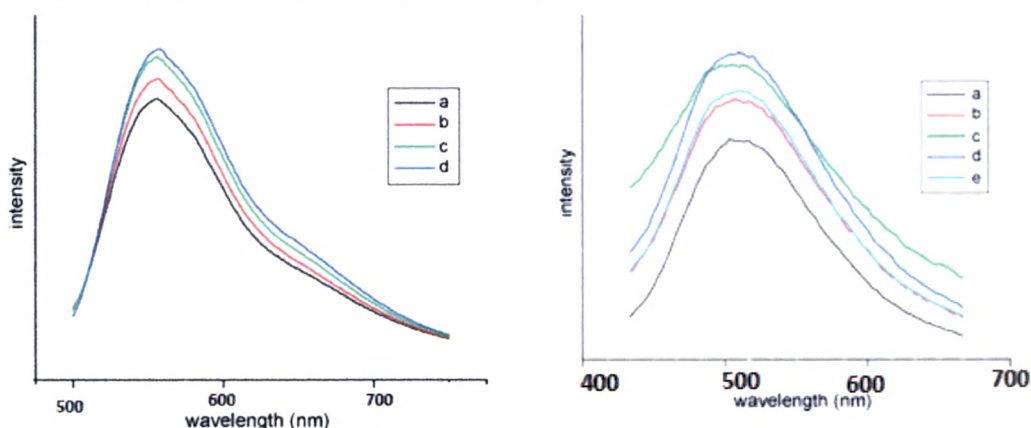


**Figure 5A.8: Stability study of gold nanoparticles synthesized using different concentrations of gellan gum,  $t = 3$  months, (a) 2-8°C (refrigerated) and (b) 25°C/65% RH (room temperature).**

The stability of nanoparticles monitored over three months showed that AuNPs synthesized using concentrations of GG (0.02% w/v to 0.1% w/v) had no shift in surface plasmon peak, indicating that nanoparticles formed were stable and without aggregation during stability period. Thus, the long term stability at higher concentration could be attributed to the GG being wrapped around AuNPs which helped in maintaining the shape and size of the nanoparticles during the period of study without any aggregation.



Development of protocols for the synthesis of water dispersible nanoparticles has immense application in catalysis, sensors, molecular markers and in particular biological applications such as biolabeling, biosensing and drug delivery.<sup>[21]</sup> Selvakannan et al., reported that capping aqueous AuNPs with the amino acid lysine stabilized the particles in solution electrostatically and also rendered them water dispersible.<sup>[22]</sup> The lysine capped AuNPs may also be obtained in the form of a dry powder after evaporation of the aqueous component, this powder being extremely stable in air and readily redispersible in water. Selvakannan et al., also reported that the amino acid tryptophan spontaneously reduces aqueous chloroaurate ions leading to the formation of tryptophan protected AuNPs that may be obtained in the form of a dry powder and readily redispersed in water.<sup>[23]</sup> The water elimination from the aqueous dispersion to achieve a dried form helps to overcome the stability limitations and improve the shelf life of nanoparticle preparations. To obtain dry powder of GG reduced AuNPs, we choose spray drying technique over other techniques. The spray drying technique exhibits advantages like low price, ease of scale up and preparation of free flowing powder. Compared to freeze drying, spray drying takes less time and is a cost effective process.<sup>[24]</sup> The dialyzed 0.02% w/v GG reduced AuNPs was spray dried to obtain ruby red colored free flowing powder [Figure 5A. 9(a)]. The SD-GG-AuNPs were then redispersed in water and characterized. Figure 5A. 9(b) shows the UV/Vis absorption spectra of redispersed AuNPs dispersion. A sharp absorption band can clearly be seen in the figure centered at 520 nm. It was similar to the AuNPs dispersion before spray drying [Figure 5A. 2(a)]. There was neither peak shift nor any additional peak, which confirmed that the spray drying had no effect on the AuNPs stability and the SD- GG-AuNPs were free from any aggregation.

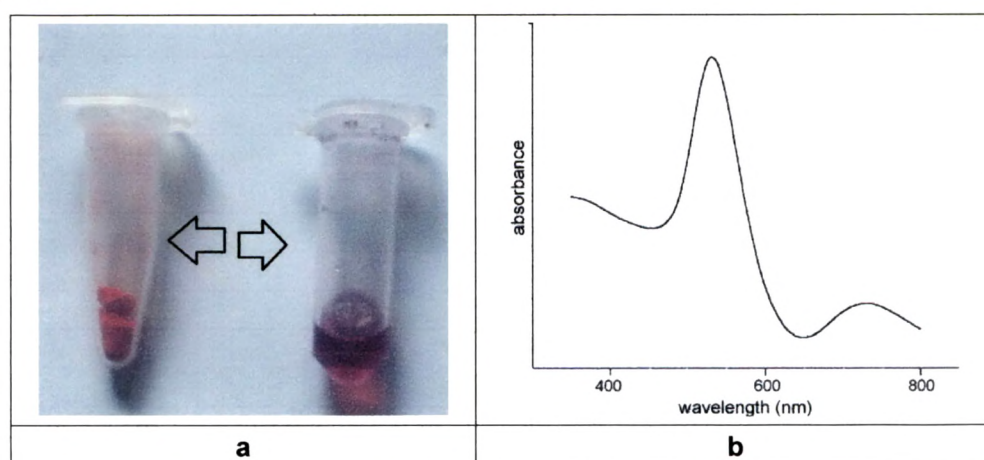


**Figure 5A.9: (a) Spray dried powder (reduced by 0.02% wlv gellan gum) and redispersed gold nanoparticles. (b) UVIVis absorption spectra of redispersed spray dried gold nanoparticles.**

The TEM image of SD-GG-AuNPs showed that the nanoparticles were spherical in shape and well dispersed [Figure 5A.10 (a)]. The overall assembly of the nanoparticles was not affected after spray drying of the AuNPs dispersion. There was no change in the shape, size and particle size distribution of the SD-GG- AuNPs. The particle size distribution of redispersed SD-GG-AuNPs [Figure 5A. 10(b)] revealed that the average size of the nanoparticles was 15 nm.

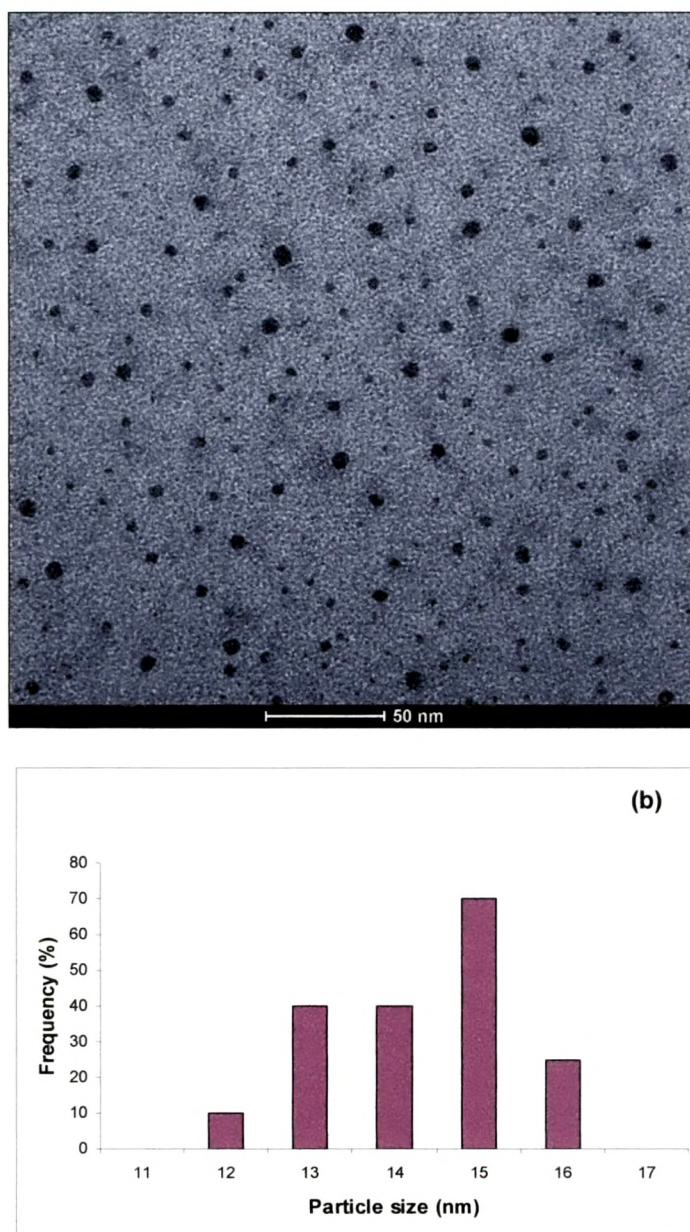


**Figure 5A.10: (a) TEM image of redispersed spray dried gold nanoparticles (reduced by 0.02% wlv gellan gum) and (b) particle size distribution of the same.**

The average particle size was same in comparison to the 0.02% w/v GG reduced AuNPs [Figure 5A. 5(e)]. The TEM and particle size distribution also concluded that the SD-GG-AuNPs formed were uniform in shape, size and free of aggregation. The SD-GG-AuNPs was monitored over a period of three months using UV/Vis spectroscopy. It was found that the spray dried powder was stable at both 25°C/65% RH (room temperature) and 2-8°C (refrigerated) during its storage period of 3 months [Figure 5A.11].

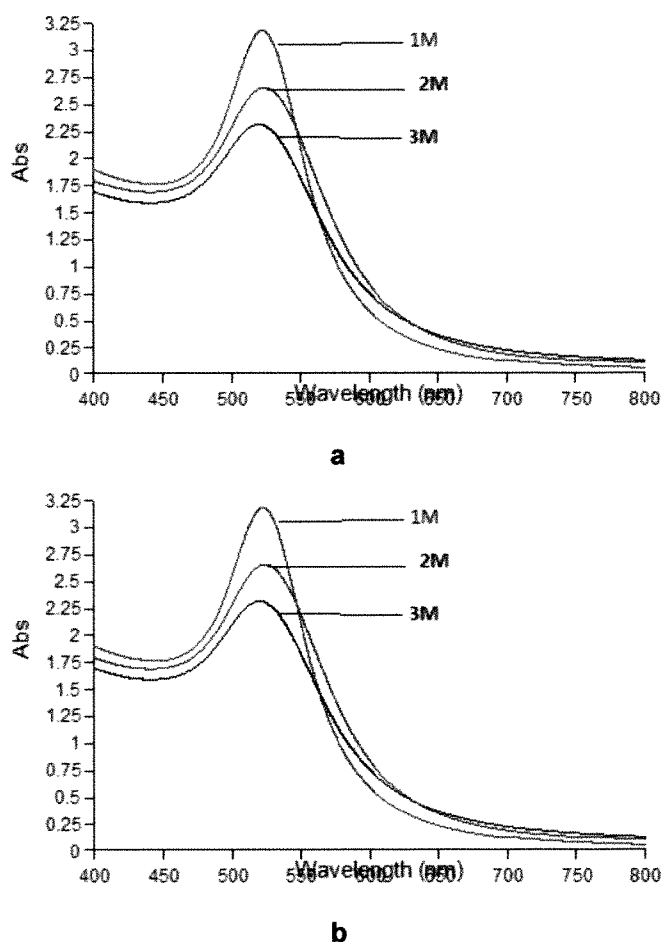


**Figure 5A.11: Stability study of redispersed spray dried gold nanoparticles (reduced by 0.02% w/v gellan gum, up to three months (a) 2-8°C (refrigerated) and (b) 25°C/65% RH (room temperature)).**

It was remarkable that the GG capping around the AuNPs remained intact even in the solid state and reconstituted easily in aqueous media without the loss of their nanoparticulate properties. The long term stability could be attributed to the stability properties of GG. It can be concluded that AuNPs dispersion can be simply stored as powdered form without compromising the stability as well as properties of the nanoparticles and can be used for biological application.



## Part B: Cellular uptake and in vivo oral toxicity studies of gellan gum reduced gold nanoparticles

### 5B.1 Outline of the present work

It is the small size of the AuNPs that makes it so useful in medicine, but it is also one of the main reasons that might make them potentially dangerous to human health. It is recognized that as particles get smaller, the surface area increases. Nanoparticles, therefore, have a much larger surface area per unit mass compared with larger particles. This increase in the surface-to-volume ratio results in the increase of the particle surface area and may render them very reactive in the cellular environment.<sup>[25]</sup> When nanoparticles come in contact with cells, the nanoparticles may get stored in the perinuclear compartment, close to or inside the cell nucleus. The nanoparticles reactivity towards cells may be desirable e.g., drug carrier or penetration of cellular barriers, or sometimes undesirable, leading to toxicity, induction of oxidative stress or cellular dysfunction and inflammation etc. So far research has focused on synthesis of AuNPs and not many studies have been focused on toxicity effect of these nanoparticles on human health. There is less information available on the effect of size, shape, surface modification and functional moieties on the bioavailability, uptake, distribution, metabolism, degradation and toxicity of AuNPs. Reports indicate that surface chemistry plays significant role in conferring the biocompatible nature of nanoparticles. Shukla et al., studied the biocompatibility of AuNPs and their endocytotic fate inside cell and conclude that the AuNPs capped by lysine and poly-L-lysine were biocompatible.<sup>[26]</sup> Connor et al., studied the cytotoxicity of gold spheres with different diameters and of different surface modifiers on leukemia K562 cells.<sup>[27]</sup> The spherical AuNPs with a variety of surface modifiers were not toxic to human cells, despite being taken up into cells. Other reports indicate that the toxic effects may be related to the nature of gold, nanoparticle size and the cell lines used. There have been claims that nanoparticles can cross the blood brain barrier in humans and AuNPs can move across the placenta from mother to fetus.<sup>[28]</sup> Studies were conducted on toxicity of AuNPs functionalized with cationic and anionic side chains. The studies showed that cationic particles were moderately toxic, whereas anionic particles were nontoxic.<sup>[29]</sup> Early work by C. Smith demonstrated the widespread distribution of particles in the body, thus highlighting the tracking of systems as an essential consideration during early clinical studies.<sup>[30]</sup> Nanoparticles can be absorbed via M cells of the gut associated lymphoid tissues as a consequence both beneficial and adverse possibilities can be encountered.<sup>[31]</sup> Citrate capped gold nanospheres were found to be non cytotoxic to baby hamster kidney and human hepatocellular liver carcinoma cells, but cytotoxic to a human carcinoma lung cell

line.<sup>[32]</sup> Hillyer et al., studied quantitative and qualitative gastrointestinal uptake and subsequent tissue/organ distribution of 4, 10, 28 and 58 nm diameter metallic colloidal gold particles following oral administration in mice.<sup>[33]</sup> Quantitative studies indicated that colloidal gold uptake was dependent on particle size: smaller particles crossing the gastrointestinal tract more readily. The principal challenge of AuNPs as a carrier system is to be biocompatible, non toxic, stable under various physiological conditions and their ability to release the active molecule to appropriate site for action when needed. As the final destination of AuNPs for drug delivery and other biomedical applications is *in vivo*, it becomes necessary to study in detail the *in vivo* toxicity for better understanding of the correlation between nanoparticles diameter, surface chemistry, interactions and transport, leading to the best possible choice of systems for drug delivery and diagnosis applications. This part of the chapter describes the cellular uptake and *in vivo* oral toxicity of the gellan gum reduced AuNPs (GG-AuNPs). The cellular uptake of AuNPs was studied on human glioma cell line, LN-229. In case of oral toxicity studies, the GG reduced AuNPs were administered orally to male and female rats for a period of 28 days. At the end of study, blood samples were collected for haematological and biochemical analysis for histopathological analysis, GG-AuNPs treated organs were assayed for any signs of toxicity.



**5B.2 Experimental work****5B.2.1 Synthesis and characterization of gellan gum reduced gold nanoparticles**

The GG-AuNPs were synthesized and characterized by UV/Vis/NIR spectroscopy (5A 5.3). The AuNPs dispersion was thoroughly dialyzed (dialysis tubing 12 kDa cut off) for 24 h to remove the byproducts of the reaction. The concentration of gold in the above sample was determined by atomic absorption spectrophotometer.

**5B.2.2 Cellular uptake of gold nanoparticles**

**5.B.2.2.A Synthesis of Texas red labeled gold nanoparticles:** The GG-AuNPs were labeled by addition of excess Texas red (140 ng/ $\mu$ L in DMSO). The colloidal dispersion was incubated overnight in darkness at 4°C to avoid photo degradation of Texas red molecules. Free Texas red in the AuNPs dispersion was removed by centrifugation at 10,000 rpm for 10 min followed by washings with carbonate buffer (pH 8.4). This effectively removed any loosely bound Texas red to the nanoparticles. The pellets containing Texas red labeled AuNPs were redispersed in carbonate buffer and used for further studies. The amount of carbonate buffer in which the pellets were redispersed was adjusted such that the surface plasmon peak intensity of the AuNPs dispersion obtained before and after centrifugation was same.

**5.B.2.2.B Cell culture and cellular uptake:** Human glioma cell line LN-229 (procured from American type culture collection, ATCC, USA) was cultured in Duibecco's modified eagle's medium (DMEM) supplemented with 1.5 gm<sup>-1</sup> sodium bicarbonate, 4 Mm glutamine and 10% fetal bovine serum. The cultures were maintained in a humidified atmosphere of 5% CO<sub>2</sub> at 37°C. For uptake of GG- AuNPs, the cells were seeded at concentration of 3x10<sup>3</sup> in 500  $\mu$ L of media on glass cover slips in a 24 well plate and incubated for 24 h to allow for adherence of the cells. After 24 h, when the cells were attached to the surface of the cover slips as a monolayer, culture medium were replaced with 500  $\mu$ L of solution containing fresh medium and Texas red labeled GG-AuNPs. The cells were further incubated for 24 h at 37°C and 5% CO<sub>2</sub> in a humidified environment.

**5.B.2.2.C Confocal laser scanning microscopy:** After incubation, the cover slips were washed extensively with ice-cold phosphate buffered saline (PBS) and fixed in 4% paraformaldehyde for 10 min at room temperature. After repeated rinses in PBS, cells were blocked in 5% BSA in PBS for 30 min at room temperature. Later the cells were again washed in PBS in dark and then the nucleus was counterstained with 4'-6-Diamidino-2-phenylindole (DAPI) for 10 min and the cells were mounted onto glass slides with 1,4-diazobicyclo-2,2,2-octanex (DABCO) as mounting medium. The cover slips were then observed using confocal microscope. The images were captured by camera coupled with microscope and processed using the computer based programmable image analyzer.

### **5B.2.3 Sub-acute oral toxicity studies of gold nanoparticles**

#### **5B.2.3.A Study design**

Animal handling was performed according Good Laboratory Practice. The sub acute toxicity study was conducted as per OECD guidelines no 407.<sup>[34]</sup> The study protocol was approved by IAEC (Institutional Animal Ethical Committee) constituted as per guidelines of committee for the purpose of control and supervision of experiments on animals (CPCSEA), Government of India.

#### **5B.2.3.B Test animals, housing and feeding conditions**

Wister rats of either sex (140-180 g) were purchased from ACTREC, Mumbai, India. The animals were housed under standard conditions temperature ( $24\pm 1^{\circ}\text{C}$ ), relative humidity ( $55\pm 10\%$ ) and 12 hr light/dark cycles throughout the experiment. Animals had access to commercially available standard pellet diet and filtered water, ad libitum. Animals were acclimatized for one week prior to the initiation of treatment. During this acclimatization period, the health status of the rats was monitored daily.

#### **5B.2.3.C Body weight of animals and food intake**

Before administration of GG-AuNPs dispersion, the animals were using a calibrated balance. The weight of the animals was recorded daily throughout the experimental period at fixed time. For recording the food consumption, weighed amount of standard rat food pellets. Was placed in the food tray of the cage. The unconsumed pellets were weighed & replaced with fresh pellets in each tray every day. The time of providing the feed was fixed throughout the study.

**5B.2.3.D General observation**

Throughout the study period, animals were observed in their cages daily for mortality and signs of toxic effects. Effect of treatment on general health of the animals, body weight and behavior was also noted.

**5B.2.3.E Dosing of Gold nanoparticles to animals**

Three different doses were given to each group as shown in table 5B.1. Vehicle and AuNP's were administered by oral route using a stainless feeding needle. Maximum permissible volume to be administered was limited to 2 ml. Gold nanoparticles were redispersed in water and administered orally for 28 days at prefixed time daily.

**Table 5B.1:** Assignment of Wister rats for 28 days oral toxicity studies.

Group	Test Sample	Dose to animals	Male	Female
A	Control	Vehicle (distilled water)	5	5
B	Low	75 ppm	5	5
C	Medium	150 ppm	5	5
D	High	300 ppm	5	5

**5B.2.3.F Blood Assays**

**Haematology analysis:** At the end of the 28 days study period, the animals were fasted overnight. The following morning, each animal was anaesthetized using anaesthetic ether and blood samples were collected from the retro orbital plexus of all the rats. Blood for haematology studies was collected into two sets tubes. In one set tubes, disodium EDTA was present. A fully automatic haematology analyzer was used to measure the following parameters: hematocrit (ht), haemoglobin (Hb), red blood corpuscles count (RBC), White blood corpuscles (WBC) and differential leukocyte count (DLC). Erythrocyte sedimentation rate (ESR) was determined by Wintrobe's method.

**Biochemical analysis:** The serum was obtained by centrifugation of the whole blood at 3000 rpm for 15min. Biochemical parameters viz, alkaline phosphatase (ALP), alanine aminotransferase (ALT), aspartate aminotransferase (AST), blood sugar level (BSL), creatinine, urea, total protein, albumin, bilirubin, cholesterol were assayed by semi automated clinical chemistry analyzer. The electrolytes ( $\text{Na}^+$  and  $\text{K}^+$ ) were analyzed using electrolyte analyzer.

**5B.2.3.G Urine analysis**

Urine samples were also collected at the end of the study period and analyzed for appearance, pH, glucose, protein and blood.

**5B.2.3.H Histopathological observations**

The animal groups treated with GG-AuNPs and the control were sacrificed at the end of study and the organs such as heart, kidney, liver, brain, lungs, stomach, intestines, pancreas, spleen, urinary bladder, testis, uterus, and ovaries were rapidly dissected out, washed in sterile phosphate buffered saline and carefully weighed on an analytical balance. The isolated organs were trimmed into small pieces and preserved in 10% formalin for 24 hrs. Organ collection and preservation for histopathology was done as per SOP. The specimens were successively dehydrated with alcohol of 70, 80, and 100% each for 1 hr. Tissues were cleaned by treating with xylene each time for 1 hr. Infiltration and impugnation was done by treating twice with xylene each time for 1 hr. Infiltration and impugnation was done by treating twice with paraffine was each time for 1 hr. Paraffin "L" shaped moulds were prepared. Specimens were cut in sections of 3-5 micrometer in thickness stained by hematoxyline-eosin. The sections were mounted by use of disterene phthalate xylene. Sections from all processed tissues of control and GG-AuNPs treated groups were examined under light microscope (Nikon coolpix camera mounted on a Nikon Eclipse microscope).

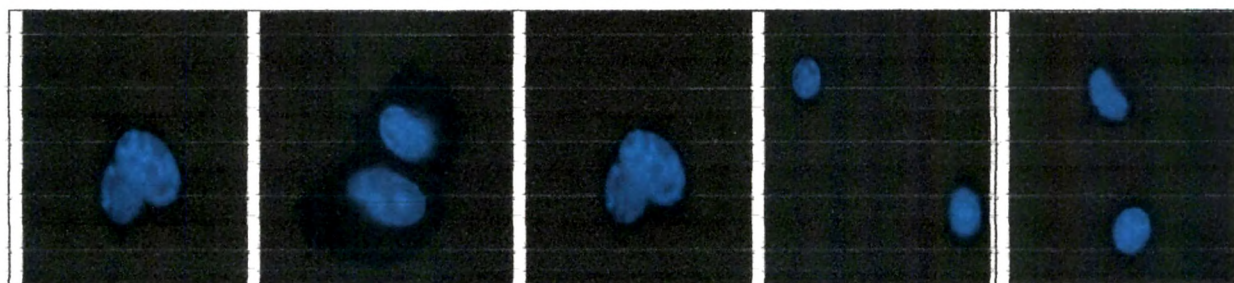
**5B.2.4 Statistical analysis**

Data of the body weight, food consumption, haematology and biochemistry values are presented as the mean  $\pm$ SD. The P values were calculated in GraphPad InStat by one way ANOVA followed by Dunnett's test by comparing different groups (control vs. treatment groups). The value of  $P < 0.05$  was considered to be statistically significant.

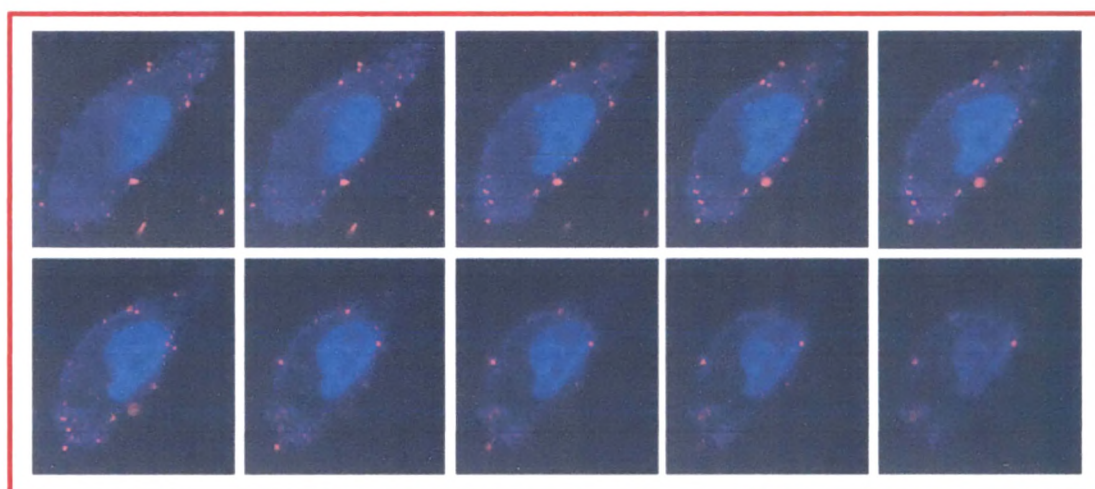
### 5B.3 Results and discussion

To understand the cellular uptake of GG-AuNPs into living cells, human glioma cells were treated with Texas red labeled GG-AuNPs. Since GG-AuNPs are non- fluorescent Texas red was conjugated with nanoparticles so that intracellular tracking of these nanoparticles could be monitored. To quantitate the amount of Texas red on AuNPs, a standard curve was plotted by measuring the fluorescence intensity of various concentrations of Texas red solutions. This was used to determine the concentration of unbound Texas red in the supernatant solution. The amount of Texas red conjugated to AuNPs was calculated to be 0.93ng/ $\mu$ L. The zeta potential of Texas red conjugated GG-AuNPs was also measured and found to be -21.35 mv. The decrease in the zeta potential from -38.25 to -21.35 mv can also be taken as an indicative of conjugation. After conjugation, the cellular uptake of labeled GG-AuNPs was studied using human glioma cell line LN-229 for 24 h. The blank GG-AuNPs were taken as control for this experiment. Figure 5B.1 shows the blank GG-AuNPs and only Texas red treated cells respectively.

(a.)



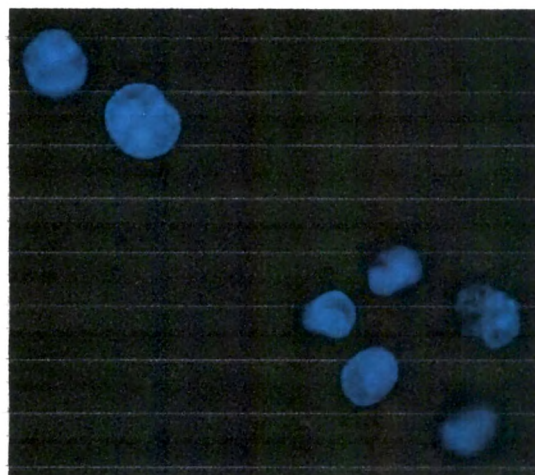
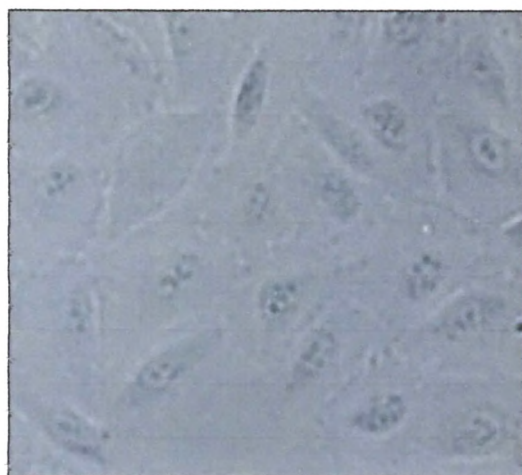
(b.)



**Figure 5B.1: Confocal images of (a) blank gold nanoparticles, (b) Texas red treated human glioma cell lines LN-229.**



It can be seen that blank GG-AuNPs treated cells were in their normal morphology and did not show any fluorescence. Gold nanoparticles are inherently non- fluorescent and hence even if they would have been taken up by the cells will not show fluorescence. In case of Texas red treated cells, no fluorescence were observed inside the cells as Texas red without any carrier cannot enter the cells. It has been well reported that the cellular uptake of the nanoparticles depends on size <sup>[35,36]</sup> and is greatly impacted by the shape of the nanoparticles.<sup>[37,38]</sup> Cellular uptake using confocal microscopy, figure 5B.2 shows that the nanoparticles were efficiently internalized by endocytosis in tumor cells within 3 h of incubation. Gold nanoparticles showed a strong fluorescence throughout the cells, indicating that a significant amount of AuNPs had entered the cells [Figure 5B. 2 (c)]. It has been reported that uptake of the nanoparticles is significantly increased for the first 2 h and the rate gradually slowed and reached a plateau at 4-7 h which again depends on the size of the nanoparticles. The reported uptake half life determined for 14 nm AuNPs was 2.10 h.<sup>[39]</sup> The nanoparticles were localized mainly in the cytoplasm and peri-nuclear region of the cells. In addition, we did not observe any of the AuNPs inside the nucleus even after 24 h of incubation. Several recent studies have shown that when nanoparticles are internalized in cells through endocytotic process, they tend to converge in the perinuclear area.<sup>[40]</sup>





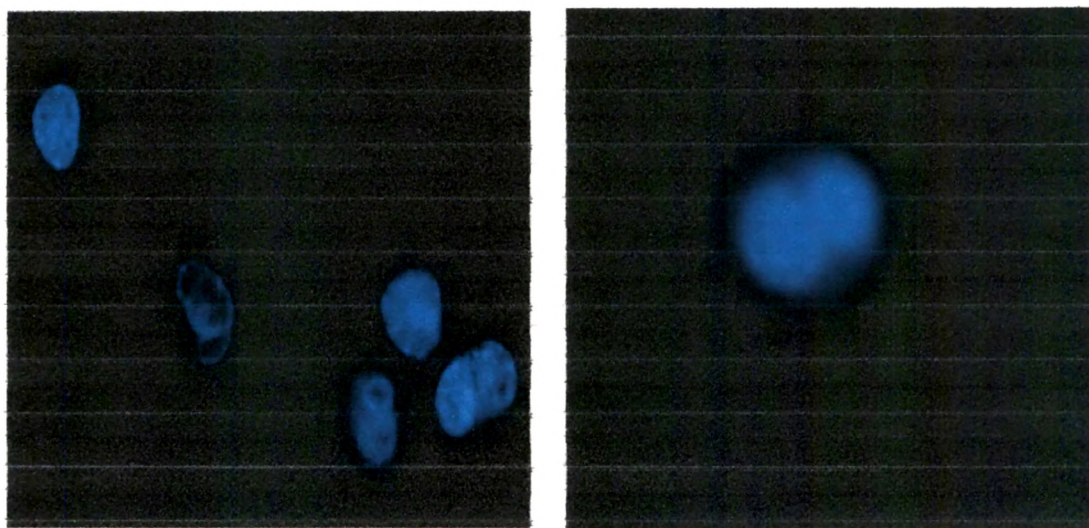


**Figure 5B.2:** Confocal images of cellular uptake of gellan gum gold nanoparticles in human glioma cell lines LN-229. (a) Phase (b) DAPI (c) gold nanoparticles and (d) overlaid.

The long history of AuNPs use for therapeutic purposes suggests that AuNPs should be biocompatible. The considerable potential use of AuNPs in nanomedicine, especially for imaging, diagnostic and therapy are supposed to improve the quality and performance of many products. This will increase the exposure of nanoparticles to public, so it becomes necessary to test out the impact of these nanoparticles on human and environment. For any type of clinical applications, it becomes very important to know about the biocompatibility and fate of these nanoparticles. The cytotoxicity of AuNPs, i.e. their cellular toxicity, has been examined by several research groups and reviewed.<sup>[41,42]</sup> But before imaging, diagnosis and therapeutic applications of AuNPs, it becomes necessary to study the *in vivo* toxicity of the same. We synthesized AuNPs using GG and evaluated the toxicity of the same by carrying out sub-acute oral toxicity in rats, which is well accepted to bring forth any toxicity on long term feeding. For 28 day sub-acute toxicity studies, the rats were randomly assigned to four groups. The three experimental groups, consisting of 10 animals each, five males and five females, received different concentration of AuNPs (75 ppm, 150 ppm and 300 ppm). The animals were observed daily for any signs of morbidity and mortality. Detailed physical examinations for signs of morbidity were conducted every week during the study period. It was observed that the animals fed with different concentrations of AuNPs were healthy. No unusual changes in behavior or in locomotors activity, no ataxia and no signs of intoxication were observed during the 28 day study period. No dose related changes in motor activity was found. The eye examinations did not reveal any dose related eye abnormalities. No mortality occurred during the study period.

**Table 5B.2:** Effect of gellan gum reduced gold nanoparticles on body weight of male rats during 28 days study period.

Group	Animal Body Weight (g) Male		
	0 <sup>th</sup> day	28 <sup>th</sup> day	Differences
Control	167.50 ± 6.45	212.50 ± 17.07	45.00
Low (75 ppm)	165.25 ± 2.06	210.75 ± 6.99	45.50
Medium (150 ppm)	170.00 ± 3.16	228.75 ± 16.15	58.75
High (300 ppm)	168.00 ± 7.25	230.25 ± 14.99	62.25

All the animals showed normal weight gains during the study period. There was no statistically significant difference ( $P>0.05$ ) in increase in body weight between the control group and experimental groups (Table 5B.2, 5B.3) indicating that different concentrations of GG-AuNPs did not alter the weight of animals.

**Table 5B.3:** Effect of gellan gum reduced gold nanoparticles on body weight of female rats during 28 days study period.

Group	Animal Body Weight (g) Female		
	0 <sup>th</sup> day	28 <sup>th</sup> day	Differences
Control	157.25 ± 5.25	200.75 ± 8.99	43.50
Low (75 ppm)	144.00 ± 4.69	180.50 ± 21.7	36.50
Medium (150 ppm)	147.00 ± 6.00	179.25 ± 9.81	32.25
High (300 ppm)	152.25 ± 11.5	194.50 ± 6.40	42.25

**Table 5B.4:** Effect of gellan gum reduced gold nanoparticles on food consumption of rats during 28 days study period.

Group	Food Consumption (g/100g of animal)			
	Male		Female	
	1 <sup>st</sup> day	28 <sup>th</sup> day	1 <sup>st</sup> day	28 <sup>th</sup> day
Control	14.19 ± 0.54	10.38 ± 0.88	11.93 ± 0.40	9.17 ± 0.41
Low (75 ppm)	13.50 ± 0.54	9.96 ± 0.34	13.02 ± 0.41	10.05 ± 1.35
Medium (150 ppm)	13.96 ± 0.26	9.42 ± 0.70	12.59 ± 0.50	9.88 ± 0.59
High (300 ppm)	14.45 ± 0.61	9.58 ± 0.64	12.15 ± 0.96	9.10 ± 0.27

The GG-AuNPs of various concentrations did not have any effect on food consumption as food consumption of the animals in the control and experimental groups was similar (Table 5B.4).

One of the most common *in vivo* toxicity assays is to examine blood composition; cell type and serum chemistry, with and without exposure to nanoparticles.<sup>[43]</sup> The deviation, either increase or decrease in blood constituents, from the control is representative of any toxicity of the nanoparticles on the animals. In the case of haematology, cell population, such as red and white blood cells or specific consideration of cells is considered during the studies. Haematological parameters viz; hematocrit (Table 5B.5), haemoglobin concentration (Table 5B.6), red blood corpuscles count (Table 5B.7), white blood corpuscles count (Table 5B.8), erythrocyte sedimentation rate (Table 5B.9) and differential leukocyte count (Table 5B.10, 5B.11) in both control and experimental groups were conducted.

**Table 5B.5:** Effect of gellan gum reduced gold nanoparticles on hematocrit level in rats after 28 days treatment.

Group	Hematocrit (%) (Mean $\pm$ SD)	
	Male	Female
Control	38.90 $\pm$ 3.47	32.35 $\pm$ 2.68
Low (75 ppm)	38.15 $\pm$ 7.56	34.70 $\pm$ 1.41
Medium (150 ppm)	36.00 $\pm$ 2.51	31.75 $\pm$ 2.35
High (300 ppm)	36.15 $\pm$ 0.81	34.92 $\pm$ 0.41

There was no significant difference ( $P>0.05$ ) and all the values were found within the normal range with no difference between the control and experimental groups.<sup>[44]</sup> White blood corpuscles count was decreased in case of male medium dose (150 ppm) comparison to the control. However, the decreased level was considered to be of no toxicological significance ( $P>0.05$ ). These results suggested that GG-AuNPs were non toxic as they did not affect the circulating red cells, nor hematopoiesis and leucopoiesis that could otherwise have caused haematological disorders.<sup>[45]</sup> These results also indicated that the normal metabolism of the animals was not affected by the administration of GG-AuNPs to animals.

**Table 5B.6:** Effect of gellan gum reduced gold nanoparticles on haemoglobin level in rats after 28 days treatment.

Group	Hemoglobin (gm/dL) (Mean $\pm$ SD)	
	Male	Female
Control	15.62 $\pm$ 1.54	13.55 $\pm$ 1.69
Low (75 ppm)	15.20 $\pm$ 3.00	13.77 $\pm$ 2.19
Medium (150 ppm)	13.97 $\pm$ 0.59	12.52 $\pm$ 1.63
High (300 ppm)	14.42 $\pm$ 0.72	14.87 $\pm$ 0.09

**Table 5B.7:** Effect of gellan gum reduced gold nanoparticles on red blood corpuscles (RBC) count in rats after 28 days treatment.

Group	Hemoglobin (gm/dL) (Mean $\pm$ SD)	
	Male	Female
Control	7.28 $\pm$ 0.68	5.87 $\pm$ 0.22
Low (75 ppm)	7.46 $\pm$ 1.70	6.11 $\pm$ 0.56
Medium (150 ppm)	6.92 $\pm$ 0.44	5.79 $\pm$ 0.55
High (300 ppm)	6.97 $\pm$ 0.23	6.58 $\pm$ 0.06

**Table 5B.8:** Effect of gellan gum reduced gold nanoparticles on white blood corpuscles (WBC) count in rats after 28 days treatment.

Group	WBC (million/cmm) (Mean $\pm$ SD)	
	Male	Female
Control	13275 $\pm$ 1757.6	9575. $\pm$ 942.96
Low (75 ppm)	11950 $\pm$ 5245. 0	14150. $\pm$ 6267
Medium (150 ppm)	7600 $\pm$ 3046.3	9675 $\pm$ 985.46
High (300 ppm)	12350 $\pm$ 2295.6	8675 $\pm$ 1358.0

**Table 5B.9:** Effect of gellan gum reduced gold nanoparticles on erythrocyte sedimentation rate (ESR) in rats after 28 days treatment.

Group	WBC (million/cmm) (Mean $\pm$ SD)	
	Male	Female
Control	2.00 $\pm$ 0.81	1.50 $\pm$ 0.57
Low (75 ppm)	1.50 $\pm$ 0.57	2.00 $\pm$ 0.81
Medium (150 ppm)	2.50 $\pm$ 0.57	2.50 $\pm$ 1.29
High (300 ppm)	1.50 $\pm$ 0.57	1.75 $\pm$ 0.50



**Table 5B.10:** Effect of gellan gum reduced gold nanoparticles on differential leucocyte count (DLC) in male rats after 28 days treatment.

Groups	Differential Leucocytes Count (%) (Mean $\pm$ SD) Male				
	Neutrophils	Lymphocytes	Eosinophils	Monocytes	Basophils
Control	21.00 $\pm$ 9.27	73.50 $\pm$ 9.32	1.50 $\pm$ 0.57	4.00 $\pm$ 0.81	0.00
75 ppm	27.50 $\pm$ 24.8	73.50 $\pm$ 9.32	2.50 $\pm$ 0.57	3.75 $\pm$ 0.95	0.00
150 ppm	14.75 $\pm$ 2.50	79.75 $\pm$ 3.77	1.50 $\pm$ 1.29	4.00 $\pm$ 2.16	0.00
300 ppm	15.25 $\pm$ 2.98	79.00 $\pm$ 3.26	1.25 $\pm$ 0.50	4.50 $\pm$ 0.57	0.00

**Table 5B.11:** Effect of gellan gum reduced gold nanoparticles on differential leucocyte count (DLC) in female rats after 28 days treatment.

Groups	Differential Leucocytes Count (%) (Mean $\pm$ SD) Male				
	Neutrophils	Lymphocytes	Eosinophils	Monocytes	Basophils
Control	20.25 $\pm$ 4.34	74.25 $\pm$ 4.19	2.25 $\pm$ 0.95	3.25 $\pm$ 1.25	0.00
75 ppm	16.75 $\pm$ 6.44	77.25 $\pm$ 6.18	1.75 $\pm$ 0.50	4.25 $\pm$ 1.50	0.00
150 ppm	16.25 $\pm$ 4.57	83.50 $\pm$ 4.65	1.75 $\pm$ 0.95	4.50 $\pm$ 1.29	0.00
300 ppm	15.50 $\pm$ 4.50	78.25 $\pm$ 4.19	2.00 $\pm$ 1.15	4.25 $\pm$ 0.95	0.00

The biochemical tests are used for diagnosis of diseases of heart, liver, kidney, etc. They are also widely used in monitoring the response of animals to toxic materials. The elevated levels indicate the occurrence of liver damage, ischemic heart disease, acute coronary syndromes, etc. Liver enzymes are normally found within the cells of the liver. If the liver is injured or damaged, the enzymes levels increase due to leaking of the enzymes in the blood.

**Table 5B.12:** Effect of gellan gum reduced gold nanoparticles on liver enzymes of male rats after 28 days treatment.

Group	Liver Enzymes (Mean $\pm$ S.D.) Male		
	Aspartate aminotransferase (IU/L)	Alanine aminotransferase (IU/L)	Alkaline aminotransferase (IU/L)
Control	227.75 $\pm$ 19.55	65.25 $\pm$ 12.2	412.00 $\pm$ 132.1
Low (75 ppm)	256.50 $\pm$ 35.06	73.25 $\pm$ 7.45	472.00 $\pm$ 56.50
Medium(150 ppm)	263.75 $\pm$ 32.98	72.75 $\pm$ 6.60	407.75 $\pm$ 143.45
High (300 ppm)	234.00 $\pm$ 25.96	67.75 $\pm$ 3.30	287.75 $\pm$ 90.72

**Table 5B.13:** Effect of gellan gum reduced gold nanoparticles on liver enzymes of female rats after 28 days treatment.

Group	Liver Enzymes (Mean $\pm$ S.D.) Female		
	Aspartate aminotransferase (IU/L)	Alanine aminotransferase (IU/L)	Alkaline phosphatase (IU/L)
Control	285.50 $\pm$ 96.86	62.00 $\pm$ 4.69	414.25 $\pm$ 78.26
Low (75 ppm)	258.00 $\pm$ 21.43	65.50 $\pm$ 7.04	378.75 $\pm$ 90.60
Medium(150 ppm)	302.00 $\pm$ 59.14	89.75 $\pm$ 43.80	370.75 $\pm$ 162.30
High (300 ppm)	232.75 $\pm$ 16.02	56.75 $\pm$ 2.21	224.50 $\pm$ 36.99

Tests conducted for the presence of liver enzymes (aspartate aminotransferase, alanine aminotransferase and alkaline phosphate) showed no significant difference ( $P > 0.05$ ) in control and experimental groups of both male and female rats (Table 5B.12, 5B.13). Alkaline phosphatase levels were decreased in case of high dose (300 ppm) in both male and female rats. However, these decreased levels were considered to be of no toxicological significance in comparison to the respective control group ( $P > 0.05$ ).

The levels of blood glucose were not significantly different ( $P>0.05$ ) between the control and experimental groups of both male and female rats (Table 5B. 14).

**Table 5B.14:** Effect of gellan gum reduced gold nanoparticles on blood sugar level (BSL) in rats after 28 days treatment.

Group	WBC (million/cmm) (Mean $\pm$ SD)	
	Male	Female
Control	133.75 $\pm$ 9.03	131.75 $\pm$ 27.0
Low (75 ppm)	115.50 $\pm$ 15.7	133.25 $\pm$ 10.30
Medium (150 ppm)	132.25 $\pm$ 16.40	131.50 $\pm$ 25.40
High (300 ppm)	133.75 $\pm$ 6.55	124.75 $\pm$ 4.78

The level of plasma analyses, such as cholesterol and bilirubin determined showed no significant difference ( $P>0.05$ ) between control and GG-AuNPs treated groups (Table 5B. 15). The levels of total protein and albumin were not significantly different ( $P>0.05$ ) between the control and experimental groups of both male and female rats (Table 5B. 16). The kidney function tests (blood urea, creatinine, sodium and potassium) showed no significant difference ( $P>0.05$ ) between the control and experimental groups of rats (Table 5B.17, 5B. 18). Feeding animals with different concentration of GG-AuNP's did not alter the functioning of the animal, indicating normal metabolism of the animals with respect to haematological and biochemical analysis.

**Table 5B.15:** Effect of gellan gum reduced gold nanoparticles on bilirubin and cholesterol on rats after 28 days treatment.

Groups	Male rats		Female rats	
	Bilirubin	Cholesterol	Bilirubin	Cholesterol
	(mg/dL) (Mean $\pm$ S.D.)			
Control	44.75 $\pm$ 4.42	52.0 $\pm$ 6.83	60.00 $\pm$ 7.07	60.75 $\pm$ 4.78
75 ppm	55.50 $\pm$ 10.90	51.0 $\pm$ 15.10	59.00 $\pm$ 5.47	58.25 $\pm$ 8.65
150 ppm	50.00 $\pm$ 2.44	58.00 $\pm$ 3.87	59.75 $\pm$ 10.10	50.00 $\pm$ 7.87
300 ppm	47.25 $\pm$ 7.22	64.00 $\pm$ 18.80	62.50 $\pm$ 4.93	57.00 $\pm$ 10.30

**Table 5B.16:** Effect of gellan gum reduced on total protein and albumin on rats after 28 days treatment.

Groups	Male rats		Female rats	
	Total Protein	Albumin	Total Protein	Albumin
	(mg/dL) (Mean $\pm$ S.D.)			
<b>Control</b>	7.47 $\pm$ 0.35	3.55 $\pm$ 0.17	8.15 $\pm$ 0.28	4.10 $\pm$ 0.45
<b>75 ppm</b>	7.50 $\pm$ 0.21	3.40 $\pm$ 0.14	7.40 $\pm$ 0.80	3.62 $\pm$ 0.25
<b>150 ppm</b>	7.87 $\pm$ 0.75	3.47 $\pm$ 0.09	8.52 $\pm$ 0.22	3.97 $\pm$ 0.18
<b>300 ppm</b>	7.20 $\pm$ 0.89	3.32 $\pm$ 0.26	8.27 $\pm$ 0.45	4.12 $\pm$ 0.39

**Table 5B.17:** Effect of gellan gum reduced gold nanoparticles on kidney function test of male rats after 28 days treatment.

Groups	Kidney Function Test (Mean $\pm$ S.D.) Male			
	Urea (mg/dL)	Creatinine (mg/dL)	Na (mmol/L)	K (mmol/L)
<b>Control</b>	78.50 $\pm$ 4.74	0.61 $\pm$ 0.02	143.0 $\pm$ 1.82	3.82 $\pm$ 0.35
<b>75 ppm</b>	77.30 $\pm$ 2.45	0.59 $\pm$ 0.13	140.70 $\pm$ 3.30	4.47 $\pm$ 0.38
<b>150 ppm</b>	74.00 $\pm$ 13.80	0.50 $\pm$ 0.01	144.50 $\pm$ 2.38	4.57 $\pm$ 0.86
<b>300 ppm</b>	75.75 $\pm$ 3.20	0.51 $\pm$ 0.05	146.0 $\pm$ 4.24	3.85 $\pm$ 0.20

**Table 5B.18:** Effect of gellan gum reduced gold nanoparticles on kidney function test of female rats after 28 days treatment.

Groups	Kidney Function Test (Mean $\pm$ S.D.) Female			
	Urea (mg/dL)	Creatinine (mg/dL)	Na (mmol/L)	K (mmol/L)
<b>Control</b>	60.60 $\pm$ 2.50	0.61 $\pm$ 0.04	141.00 $\pm$ 3.65	4.60 $\pm$ 0.84
<b>75 ppm</b>	59.37 $\pm$ 2.78	0.59 $\pm$ 0.08	140.20 $\pm$ 3.30	4.32 $\pm$ 0.38
<b>150 ppm</b>	63.67 $\pm$ 4.20	0.54 $\pm$ 0.03	144.00 $\pm$ 4.96	4.90 $\pm$ 1.02
<b>300 ppm</b>	58.00 $\pm$ 5.87	0.61 $\pm$ 0.01	142.20 $\pm$ 5.18	4.62 $\pm$ 0.46

The urine samples of the male and female rats were collected over time. The pH of urine of both male and female rats in the control and the experimental group was alkaline. In case of protein analysis, traces of protein were found in the urine. It is known that occurrence of traces proteins is a normal finding in most of the animals.

A higher concentration of proteins is considered abnormal which may be due to glomerular injury, defective tubular reabsorption etc. <sup>[46]</sup> If the kidney functioning is normal, the glucose is reabsorbed by the renal tubules. No glucose was present in urine of both male and female rats of control and the experimental groups.

Another widely utilized in vivo test is the examination of histological changes that occurs in cells/tissue/organs after exposure to nanoparticles. <sup>[43]</sup> Histological examination was performed on tissues that have been fixed after sacrifice of the exposed animal and changes in the tissue and cell morphology were assessed using light microscopy. Some of the typical tissues examined after nanoparticles exposure include: liver, kidneys, spleen, lungs and heart. <sup>[43,47]</sup>



Histopathological studies were carried out to study the effect of GG-AuNPs on the vital organs. The individual organs were weighed and it was found that there was no significant difference ( $P>0.05$ ) between the organ weight of control and treated groups (Table 5B. 19). The absence of any changes in various organs point out the fact that the GC-AuNPs did not induce any anomalous growth or inflammation of these organs which would otherwise have resulted in higher organ weight in the treated groups.

**Table 5B.19:** Effect of gellan gum reduced gold nanoparticles on organ weight of rats after 28 days treatment.

Group		Organ weight (g) (Mean $\pm$ S.D.)			
		Control	75 ppm	150 ppm	300 ppm
Heart		1.17 $\pm$ 0.33	0.98 $\pm$ 0.01	1.00 $\pm$ 0.11	0.92 $\pm$ 0.05
Kidney	Left	1.18 $\pm$ 0.13	0.88 $\pm$ 0.07	0.74 $\pm$ 0.44	1.01 $\pm$ 0.18
	Right	1.00 $\pm$ 0.14	0.95 $\pm$ 0.09	0.95 $\pm$ 0.11	0.92 $\pm$ 0.08
Liver		9.86 $\pm$ 0.73	8.84 $\pm$ 0.41	10.33 $\pm$ 1.28	9.66 $\pm$ 1.30
Lung (combined)		2.37 $\pm$ 0.71	1.72 $\pm$ 0.08	1.95 $\pm$ 0.26	1.93 $\pm$ 0.21
Pancreas		1.08 $\pm$ 0.19	1.10 $\pm$ 0.23	1.09 $\pm$ 0.38	1.10 $\pm$ 0.10
Spleen		1.33 $\pm$ 0.18	0.99 $\pm$ 0.22	1.18 $\pm$ 0.46	1.05 $\pm$ 0.14
Stomach		2.05 $\pm$ 0.13	2.01 $\pm$ 0.30	2.00 $\pm$ 0.42	1.97 $\pm$ 0.23
Intestine	Large	3.32 $\pm$ 0.58	3.73 $\pm$ 0.74	3.76 $\pm$ 0.49	3.37 $\pm$ 0.83
	Small	4.96 $\pm$ 0.90	6.28 $\pm$ 1.32	5.49 $\pm$ 1.73	6.64 $\pm$ 0.40
Brain		2.02 $\pm$ 0.14	1.87 $\pm$ 0.29	1.68 $\pm$ 0.06	1.81 $\pm$ 0.05
Urinary Bladder		0.64 $\pm$ 0.15	0.55 $\pm$ 0.09	0.51 $\pm$ 0.06	0.56 $\pm$ 0.11
Testis		2.40 $\pm$ 0.24	2.37 $\pm$ 0.08	2.70 $\pm$ 0.31	2.68 $\pm$ 0.17
Uterus		0.40 $\pm$ 0.14	0.29 $\pm$ 0.05	0.24 $\pm$ 0.10	0.35 $\pm$ 0.05
Ovaries		0.18 $\pm$ 0.05	0.18 $\pm$ 0.02	0.22 $\pm$ 0.01	0.18 $\pm$ 0.02

The histopathological findings of all the organs can be seen in figure 5B.3 to 15. Any structural changes in the organs are considered to be good indication for any sort of toxicity due to nanoparticles. The histopathology of all the organs is discussed below. <sup>[48]</sup> The absence of any pathological change in organs point out the fact that the GG-AuNPs did not induce any toxicity in animals.

**Heart:** The section of the control heart showed normal myocardium. Same findings were observed for dose 50 ppm, 150 ppm and 300 ppm. No pigment deposits were seen in any groups. Thus there was no toxic effect of GG-AuNPs on the heart (Figure 5B.3).

**Kidney:** The sections of the control rat showed normal renal cortex with normal appearing glomerular tubules and normal renal papilla. After the dose of GG-AuNPs, sections were showed renal cortex with normal appearing glomerular tubules and normal renal papilla. There were no pigment deposits in the tubules in the treated groups (Figure 5B.4).

**Liver:** The sections of the control and the GG-AuNPs treated groups showed normal hepatic architecture. The hepatocytes in the liver sample appeared normal and the portal tracts were also found to be normal in all treated groups. No inflammation was seen in the GG-AuNPs treated groups (Figure 5B.5).

**Lung:** The sections from control animals showed normal alveolar architecture. No thickening of inter alveolar septa or cellular infiltrations were observed. The same histopathological findings were observed in GG-AuNPs treated groups (Figure 5B.6).

**Pancreas:** The sections from the control and the GG-AuNPs treated groups showed normal pancreatic architecture. Pancreatic cells were observed normal in all AuNPs treated groups (Figure 5B.7).

**Spleen:** The two major functional zones of the spleen are the hematogenous red pulp and the lymphoid white pulp. The section from the control showed normal splenic architecture with normal red and white pulp. Same histopathology was observed with the GG-AuNPs treated groups (Figure 5B.8).

**Stomach:** The most conspicuous tissue feature of the stomach is the thick glandular mucosa, packed with gastric glands which secrete digestive enzymes and acid. There were no pathological changes in the mucosal lining of the control as well as the GG-AuNPs treated groups. No inflammation was observed in the treated groups. (Figured 5B.9).

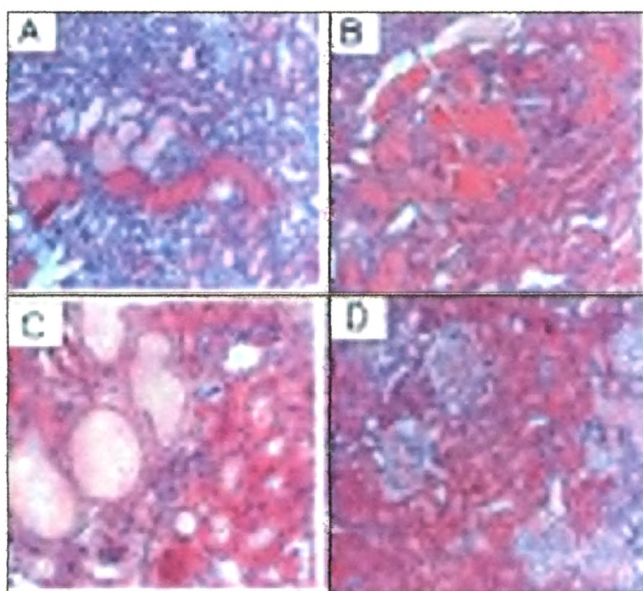


**Figure 5B.3:** Light photomicrograph of heart after 28 days of administration of gellan gum reduced gold nanoparticles by oral route at a dose of (a) control, (b) 75 ppm (c) 150 ppm and (d) 300 ppm.

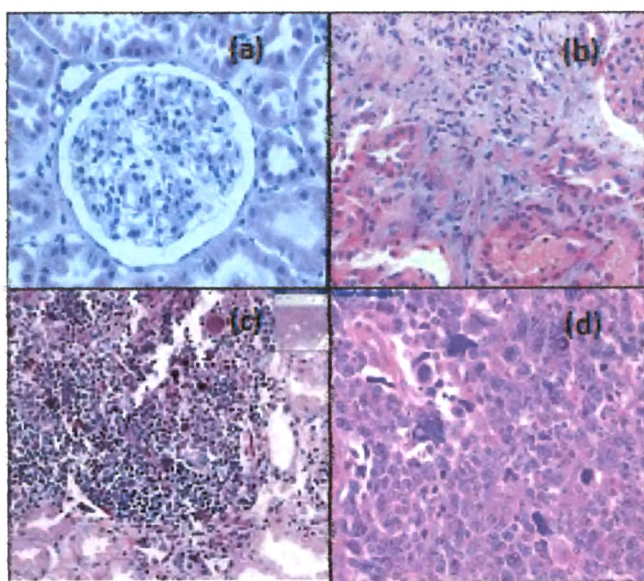


**Figure 5B.4:** Light photomicrograph of kidney after 28 days of administration of gellan gum reduced gold nanoparticles by oral route at a dose of (a) control, (b) 75 ppm (c) 150 ppm and (d) 300 ppm.



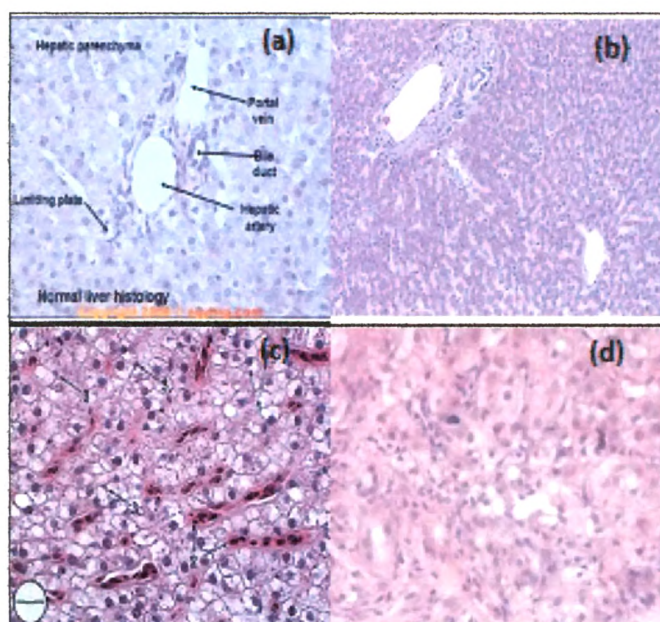


**Figure 5B.5:** Light photomicrograph of liver after 28 days of administration of gellan gum reduced gold nanoparticles by oral route at a dose of (a) control, (b) 75 ppm (c) 150 ppm and (d) 300 ppm.

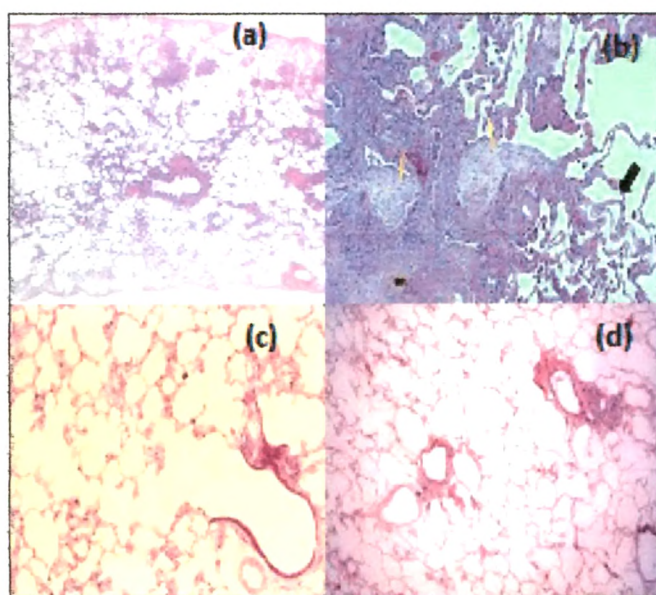


**Figure 5B.6:** Light photomicrograph of lung after 28 days of administration of gellan gum reduced gold nanoparticles by oral route at a dose of (a) control, (b) 75 ppm (c) 150 ppm and (d) 300 ppm.



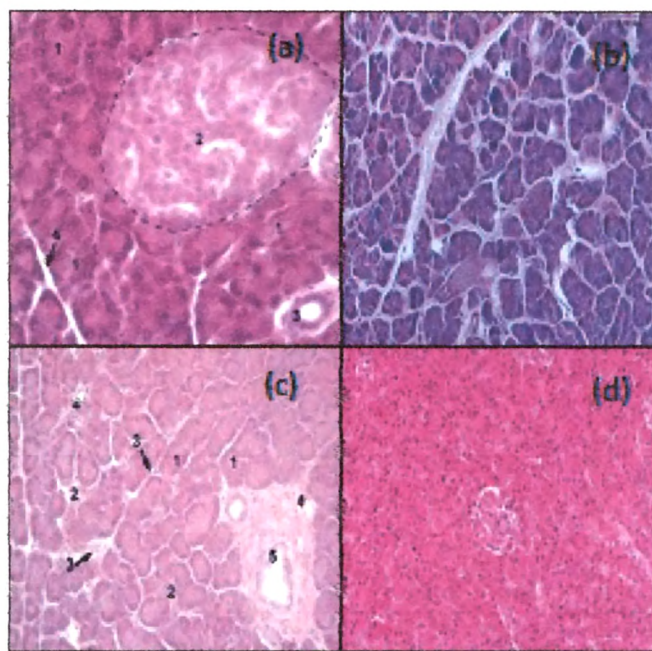


**Figure 5B.7:** Light photomicrograph of pancreas after 28 days of administration of gellan gum reduced gold nanoparticles by oral route at a dose of (a) control, (b) 75 ppm (c) 150 ppm and (d) 300 ppm.

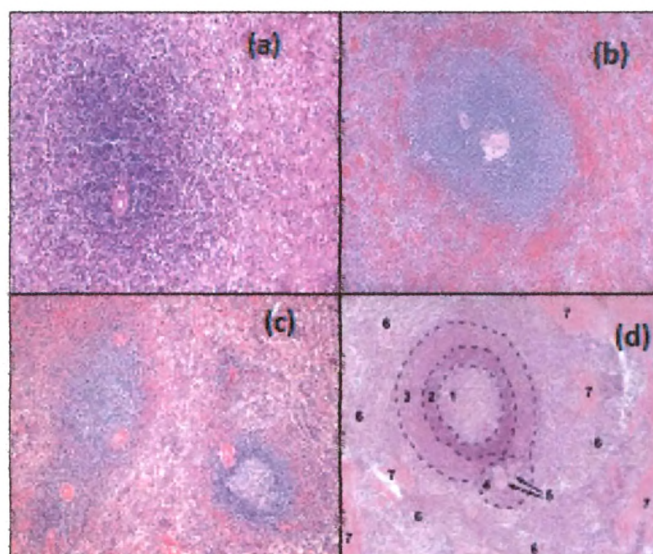


**Figure 5B.8:** Light photomicrograph of spleen after 28 days of administration of gellan gum reduced gold nanoparticles by oral route at a dose of (a) control, (b) 75 ppm (c) 150 ppm and (d) 300 ppm.

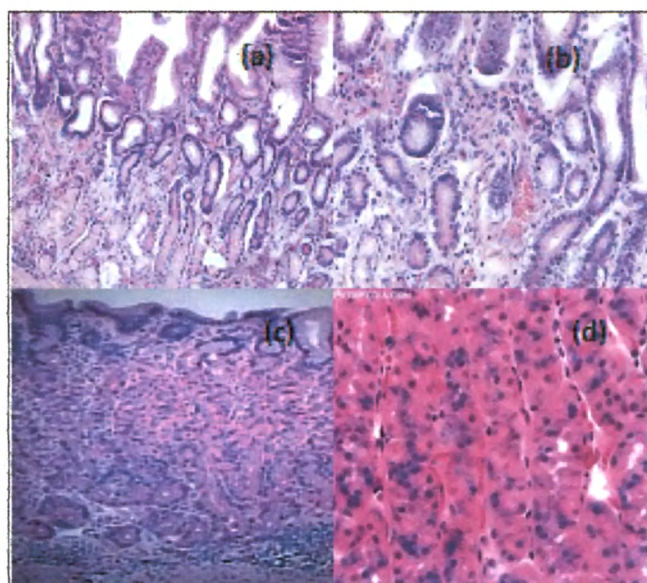


**Figure 5B.9:** Light photomicrograph of stomach after 28 days of administration of gellan gum reduced gold nanoparticles by oral route at a dose of (a) control, (b) 75 ppm (c) 150 ppm and (d) 300 ppm.

**Intestines:** There were no pathological changes in the mucosal lining of the small as well as large intestine in the control group. In the GG-AuNP's treated groups (50, 150, 300 ppm), no change was observed confirming no treatment related toxicity due to AuNPs (Figure 5B.10).

**Brain:** The GG-AuNPs treated sections from the brain showed normal neuronal as well as glial elements. No morphological alteration was noted in the brain samples (control and GG-AuNPs) treated animals (Figure 5B. 11).

**Urinary Bladder:** The urinary bladder sections showed unremarkable transitional mucosa and normal underlying stroma. There was no change in the GG-AuNPs treated groups compared to the control (Figure 5B.12).



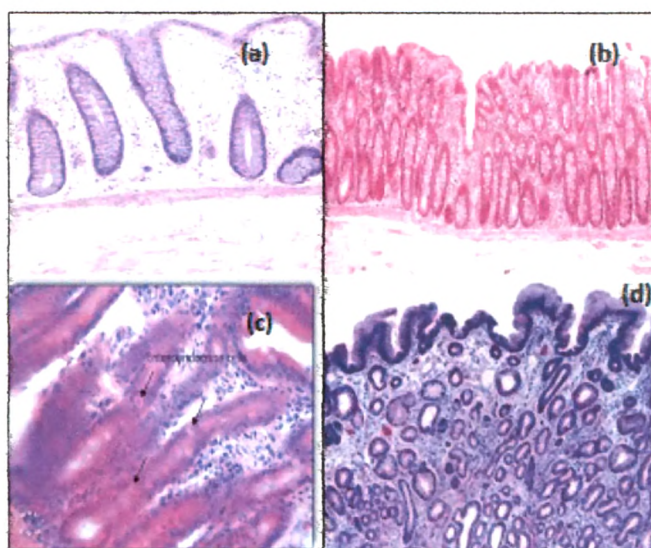


**Figure 5B.10:** Light photomicrograph of intestine after 28 days of administration of gellan gum reduced gold nanoparticles by oral route at a dose of (a) control, (b) 75 ppm (c) 150 ppm and (d) 300 ppm.

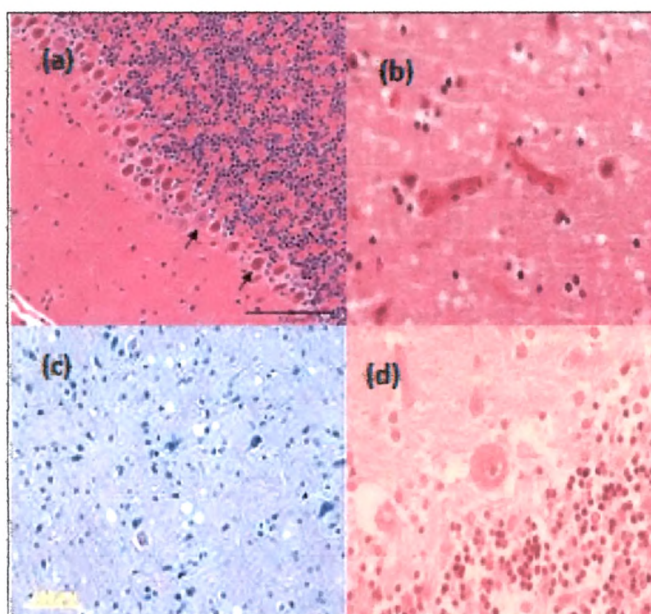


**Figure 5B.11:** Light photomicrograph of brain after 28 days of administration of gellan gum reduced gold nanoparticles by oral route at a dose of (a) control, (b) 75 ppm (c) 150 ppm and (d) 300 ppm.

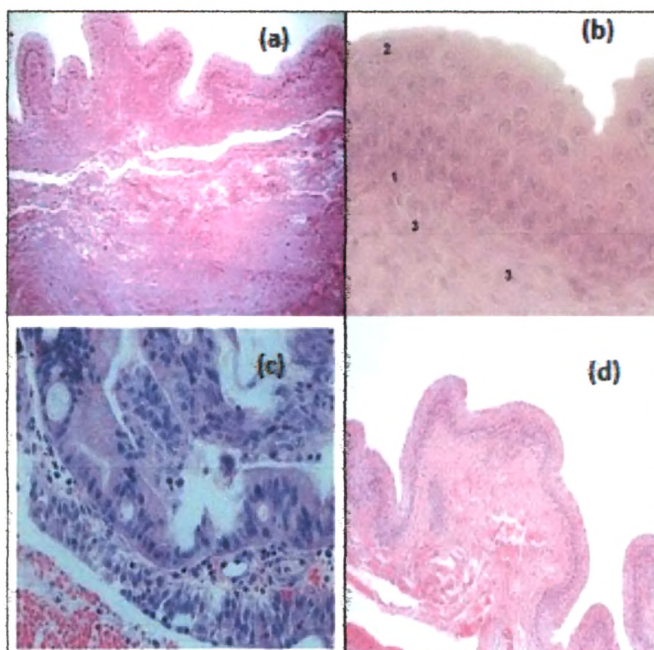


**Figure 5B.12:** Light photomicrograph of urinary bladder after 28 days of administration of gellan gum reduced gold nanoparticles by oral route at a dose of (a) control, (b) 75 ppm (c) 150 ppm and (d) 300 ppm.

**Testis:** The testis sections of the GG-AuNPs treated groups showed normal shape and size of seminiferous tubules with active spermatogenesis and maturation. The interstitium was normal. There was no pathological change observed in the GG-AuNPs treated group (Figure 5B.13).

**Uterus:** The sections of the control and the GG-AuNPs treated groups showed normal endometrium and myometrium (Figure 5B.14).

**Ovaries:** Histological examination of ovaries in the control and treated groups revealed different stages of follicular development. No abnormalities were observed in germinal epithelium, stages of follicular development. No abnormalities were observed in germinal epithelium, stages of follicular development, maturation and corpus luteum (Figure 5B.15).



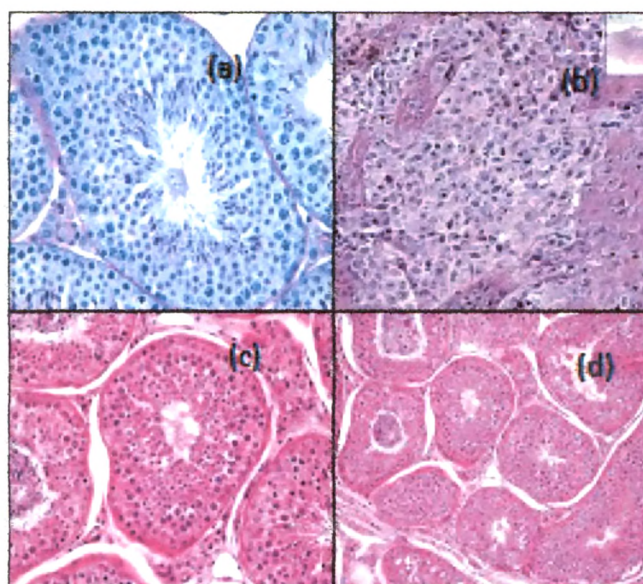


**Figure 5B.13:** Light photomicrograph of testis after 28 days of administration of gellan gum reduced gold nanoparticles by oral route at a dose of (a) control, (b) 75 ppm (c) 150 ppm and (d) 300 ppm.

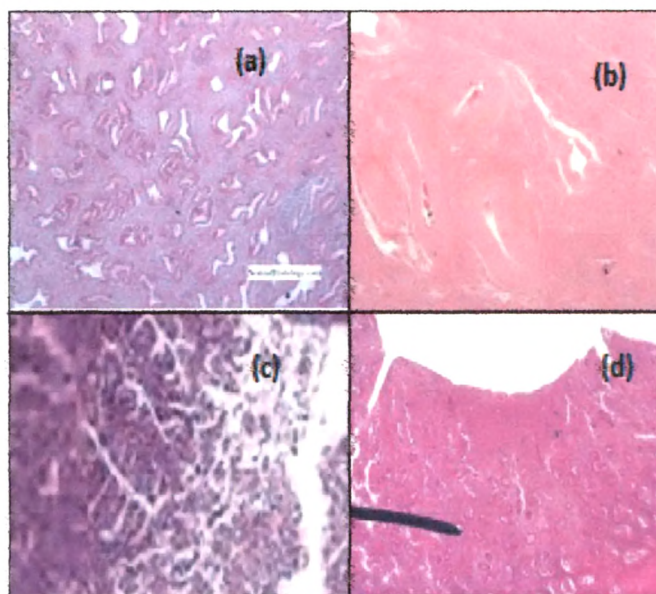


**Figure 5B.14:** Light photomicrograph of uterus after 28 days of administration of gellan gum reduced gold nanoparticles by oral route at a dose of (a) control, (b) 75 ppm (c) 150 ppm and (d) 300 ppm.



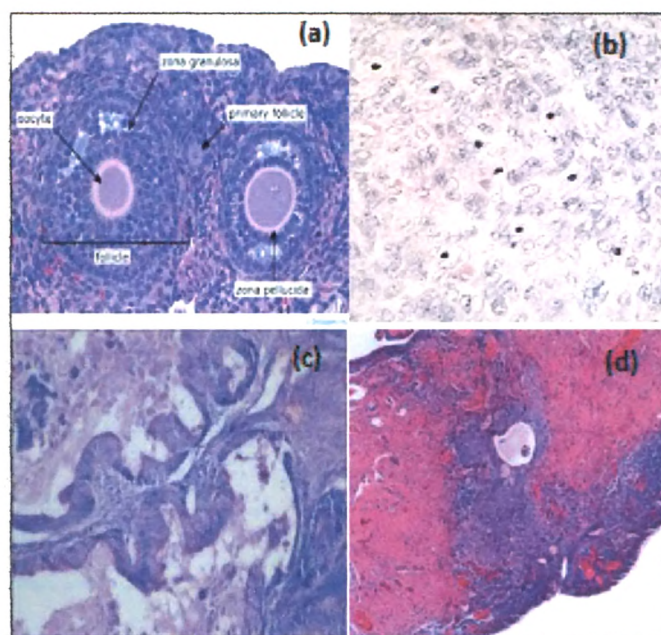


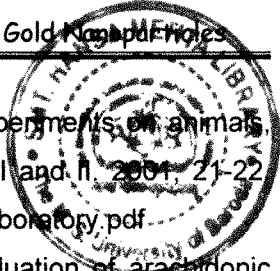
**Figure 5B.15:** Light photomicrograph of ovary after 28 days of administration of gellan gum reduced gold nanoparticles by oral route at a dose of (a) control, (b) 75 ppm (c) 150 ppm and (d) 300 ppm.

**References:**

1. C. Burda, X. Chen, R. Narayanan, M.A. El-Sayed. Chemistry and properties of nanocrystals of different shapes. *Chem. Rev.*, 2005, 105; 1025-1102.
2. P. Ghosh, G. Han, M. De, C.K. Kim, V.M. Rotello. Gold nanoparticles in delivery applications. *Adv. Drug Deliv. Rev.*, 2008, 60; 1307-1315.
3. M.C. Daniel, D. Astruc. Gold nanoparticles: Assembly, supramolecular chemistry, quantum size related properties, and applications toward biology, catalysis, and nanotechnology. *Chem. Rev.*, 2004, 104; 293-346.
4. M. Brust, M. Walker, D. Bethell, D.J. Schiffrin, R. Whyman. Synthesis of thiol-derivatised gold nanoparticles in a two-phase liquid-liquid system. *J. Chem. Soc. Chem. Commun.*, 1994, 7; 810-812.
5. C. Zandonella, Cell nanotechnology: The tiny toolkit. *Nature* 2003, 423; 10- 12.
6. A. Curtis, C. Wilkinson. Nanotechniques and approaches in biotechnology. *Trends Biotechnol.*, 2001, 19; 97-101.
7. L.L. Rouhana, J.A. Jaber, J.B. Schlenoff. Aggregation resistant water soluble gold nanoparticles. *Langmuir* 2007, 23; 12799-12801.
8. V. Kattumuri, K. Katti, S. Bhaskaran, E.J. Boote, S.W. Casteel, G.M. Fent, D.J. Robertson, M. Chandrasekhar, R. Kannan, K.V. Katti. Gum arabic as a phytochemical construct for the stabilization of gold nanoparticles: In vivo pharmacokinetics and x-ray contrast imaging studies. *Small* 2007, 3; 333- 341.
9. Kelcogel. <http://www.cpkelco.com/food/gellan.html>.
10. M.A. O'Neill, R.R. Selvendran, V.J. Morris. Structure of the acidic extracellular gelling polysaccharide produced by pseudomonas elodea. *Carbohydr. Res.*, 1983, 124; 123-133.
11. P.E. Jansson, B. Lindberg, P.A. Sandford. Structural studies of gellan gum, an extracellular polysaccharide elaborated by pseudomonas elodea. *Carbohydr. Res.*, 1983, 124; 135-139.
12. J.M. Fuente, S. Penades. Glyconanoparticles: Types, synthesis and applications in glycoscience, biomedicine and material science. *Biochem. Biophys. Acta.*, 2006, 1760; 636-651.
13. D.R. Bhumkar, H.M. Joshi, M. Sastry, V.B. Pokharkar. Chitosan reduced gold nanoparticles as novel carriers for transmucosal delivery of insulin. *Pharm. Res.*, 2007, 24; 1415-1426.
14. S. Link, M.A. El-Sayed, Size and temperature dependence of the plasmon absorption of colloidal gold nanoparticles. *J. Phys. Chem. B.*, 1999, 103; 4212-4217.

15. A.N. Shipway, M. Lahav, R. Gabai, I. Wiliner. Investigations into the electrostatically induced aggregation of Au nanoparticles. *Langmuir* 2000; 16; 8789-8795.
16. P.K. Jain, X. Huang, I.H. El-Sayed, M.A. El-Sayed. Noble metals on the nanoscale: Optical and photothermal properties and some applications in imaging, sensing, biology, and medicine. *Acc. Chem. Res.*, 2008, 41; 1578- 1586.
17. A. Martin, J. Swarbrick, A. Cammarata. Physical pharmacy. *Varghese Publishing House, Mumbai*, 1991.
18. C.J. Sunderland, M. Steiert, J.E. Talmadge, A.M. Derfus, S.E. Barry. Targeted nanoparticles for detecting and treating cancer. *Drug Dev. Res.*, 2006, 67; 70-93.
19. X. Sun, S. Dong, E. Wang. High yield synthesis of large single crystalline gold nanoplates through a polyamine process. *Langmuir* 2005, 21; 4710- 4712.
20. K. Sato, K. Hosokawa, M. Maeda. Rapid aggregation of gold nanoparticles induced by non-cross-linking DNA hybridization. *J. Am. Chem. Soc.*, 2003, 125; 8102-8103.
21. D.I. Gittins, F. Caruso. Biological and physical applications of water based metal nanoparticles synthesized in organic solution. *Chem. Phys. Chem.*, 2002, 3; 110-113.
22. P.R. Selvakannan, S. Mandal, S. Phadtare, R. Pasricha, M. Sastry. Capping of gold nanoparticles by the amino acid lysine renders them water dispersible. *Langmuir* 2003, 19; 3545-3549.
23. P.R. Selvakannan, S. Mandal, S. Phadtare, A. Gole, R. Pasricha, S.D. Adyanthaya, M. Sastry. Water dispersible tryptophan protected gold nanoparticles prepared by the spontaneous reduction of aqueous chloroaurate ions by the amino acid. *J. Colloid Interface Sci.*, 2004, 269; 97-102.
24. J. Broadhead, S.K.E. Rouan, C.T. Rhodes. The spray drying of pharmaceuticals. *Drug Dev. Ind. Pharm.*, 1992, 18; 1169-1206.
25. K. Donaldson, R. Aitken, L. Tran, V. Stone, R. Duffin, G. Forrest, A. Alexander. Carbon nanotubes: A review of their properties in relation to pulmonary toxicology and workplace safety. *Toxicol. Sci.*, 2006, 92; 5-22.
26. R. Shukla, V. Bansai, M. Chaudhary, A. Basu, R.R. Bhonde, M. Sastry. Biocompatibility of gold nanoparticles and their endocytotic fate inside the cellular compartment: A microscopic overview. *Langmuir* 2005, 21; 10644- 10654.
27. E.E. Connor, J. Mwamuka, A. Gole, C.J. Murphy, M.D. Wyatt. Gold nanoparticles are taken up by human cells but do not cause acute cytotoxicity. *Small* 2005, 1; 325-327.
28. Dangers come in small particles. Nanotech safety-Hazards magazine, 2006, 87. Available from URL: <http://www.hazards.org/nanotech/safety.htm>.

29. C.M. Goodman, T. Yilmaz, V.M. Rotello. Toxicity of gold nanoparticles functionalized with cationic and anionic side chains. *Bioconjugate Chem.*, 2004, 15; 897-900.
30. J.R.C. Smith. An electron microscopic study of injured and abnormally permeable lymphatics. *Ann. New York Acad. Sci.*, 1964, 116; 803-830.
31. N. Hussain, V. Jaitley, A.T. Florence. Recent advances in the understanding of uptake of microparticulates across the gastrointestinal lymphatics. *Adv. Drug Deliv. Rev.*, 2001, 50; 107-142.
32. H.K. Patra, S. Banerjee, U. Chaudhuri, P. Lahiri, A.K. Dasgupta. Cell selective response to gold nanoparticles. *Nanomedicine* 2007, 3; 111-119.
33. J.F. Hillyer, R.M. Albrecht. Gastrointestinal persorption and tissue distribution of differently sized colloidal gold nanoparticles. *J. Pharm. Sci.*, 2001, 90; 1927-1936.
34. OECD guidelines for the testing of chemicals. Test guideline number 407. Repeated dose 28 day oral toxicity in rodents. Organisation for Economic Co-operation and Development, Paris, 2001.
35. H. Gao, W. Shi, L.B. Freund. Mechanics of receptor mediated endocytosis. *Proc. Natl. Acad. Sci. USA* 2005, 102; 9469-9474.
36. P. Decuzzi, M. Ferrari. The role of specific and non-specific interactions in receptor mediated endocytosis of nanoparticles. *Biomaterials* 2007, 28; 2915-2922.
37. J.A. Champion, S. Mitragotri. Role of target geometry in phagocytosis. *Proc. Natl. Acad. Sci. USA* 2006, 103; 4930-4934.
38. Y. Geng, P. Dalhaimer, S. Cai, R. Tsai, M. Tewari, T. Minko, D.E. Discher. Shape effects of filaments versus spherical particles in flow and drug delivery. *Nat. Nanotechnol.*, 2007, 2; 249-255.
39. B.D. Chithrani, A.A. Ghazani, W.C.W. Chan. Determining the size and shape dependence of gold nanoparticle uptake into mammalian cells. *Nano Lett.*, 2006, 6; 662-668.
40. G. Kaul, M. Amiji. Cellular interactions and in vitro DNA transfection studies with poly (ethylene glycol) modified gelatin nanoparticles. *J. Pharm. Sci.*, 2005, 94; 184-198.
41. N. Lewinsky, V. Colvin, R. Drezek. Cytotoxicity of nanoparticles. *Small* 2008, 4; 26-49.
42. C.J. Murphy, A.M. Gole, J.W. Stone, P.N. Sisco, A.M. Alkilany, E.C. Goldsmith, S.C. Baxter. Gold nanoparticles in biology: Beyond toxicity to cellular imaging. *Acc. Chem. Res.*, 2008, 41; 1721-1730.
43. B.J. Marquis, S.A. Love, K.L. Braun, C.L. Haynes. Analytical methods to assess nanoparticle toxicity. *Analyst* 2009, 134; 425-439.

- 
44. Committee for the purpose of control and supervision on experiments on animals. CPCSEA guidelines for laboratory animal facility. Annexure I and II, 2001, 21-22. Available online at [http://envfor.nic.in/divisions/awd/cpcsea\\_laboratory.pdf](http://envfor.nic.in/divisions/awd/cpcsea_laboratory.pdf).
45. A. Nisha, S.P. Muthukumar, G. Venkateswaran. Safety evaluation of arachidonic acid rich *Mortierella alpina* biomass in albino rats: A subchronic study. *Reg. Toxicol. Pharmacol.*, 2009, 53; 186-194.
46. R.L. Halls, N.E. Everds. Principles and methods of toxicology. *Informa Healthcare, USA* 2003.
47. C.R. Patra, S.S.A. Moneim, E. Wang, S. Dutta, S. Patra, M. Eshed, P. Mukherjee, A. Gedanken, V.H. Shah, D. Mukhopadhyay. In vivo toxicity studies of europium hydroxide nanorods in mice. *Toxicol. App. Pharmacol.*, 2009, 240; 88-98.
48. B. Young, J.W. Heath. Functional histology: A text and color atlas. *Elsevier Ltd. Churchill Livingstone*, 2002.